University of Southampton

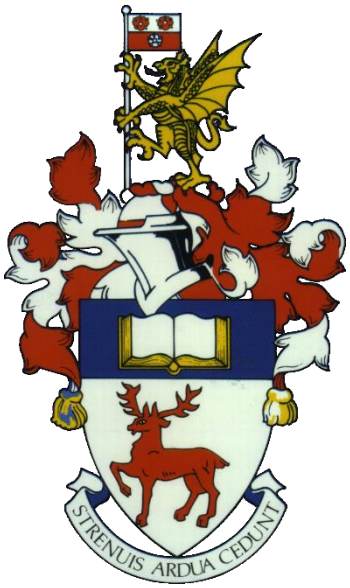

The recent morphological evolution of Pagham Harbour entrance and the cause of the breach to Church Norton spit in winter 2016

Academic supervisor: Professor Ian Townend

Industrial supervisor: Colin Scott (ABPmer)

Emma Harris

MSc Engineering in the Coastal Environment

Faculty of Engineering and the Environment

September 2017

This thesis was submitted for examination in September 2017. It does not necessarily represent the final form of the thesis as deposited in the University after examination.

Declaration

I, Emma Harris declare that this thesis and the work presented in it are my own and has been generated by me as the result of my own original research. I confirm that:

1. This work was done wholly or mainly while in candidature for a degree at this University;
2. Where any part of this thesis has previously been submitted for any other qualification at this University or any other institution, this has been clearly stated;
3. Where I have consulted the published work of others, this is always clearly attributed;
4. Where I have quoted from the work of others, the source is always given.
5. With the exception of such quotations, this thesis is entirely my own work;
6. I have acknowledged all main sources of help;
7. Where the thesis is based on work done by myself jointly with others, I have made clear exactly what was done by others and what I have contributed myself;
8. None of this work has been published before submission.

Acknowledgements

I would like to express my greatest thank you to my supervisor, Professor Ian Townend for his guidance, support and expertise in this area (and the numerous and swift updates to CoastalTools along the way). I am particularly thankful to Colin Scott at ABPmer, for his extensive knowledge on Pagham Harbour and for the very insightful site visit. I would like to extend my thanks to Nadine Warken at ABP and Nicky Dewey at ABPmer, for their help and technical GIS guidance during the GIS section of this project. I would also like to extend my thanks further to Dr Hachem Kassem and Dr Travis Mason for their additional guidance and support, and to Ivan Lang and Stephen Webster from the RSPB, for permission to collect sediment samples during my site visit in May.

Finally, I would like to thank Dr Sam Cope and the Standing Conference on Problems Associated with the Coastline (SCOPAC) committee for awarding me the 2017 Bradbury Bursary, based on the scoping study that I prepared for this thesis. I am delighted and feel incredibly honoured to receive this bursary.

Abstract

Situated on the south coast of England, Pagham Harbour is a highly dynamic ebb dominant coarse grained tidal inlet. It is characterised by a double spit system and over the past 10 years, has displayed extensive morphological changes and increasingly threatened properties along Pagham beach due to coastal erosion. Early in 2016 the Church Norton spit, also referred to as the southern spit, naturally breached, resulting in the formation of a new tidal inlet channel. The aim of this study was to determine how Pagham Harbour entrance and the spit system have evolved, following the breach of Church Norton spit in spring 2016 and to identify the cause(s) of the breach.

A series of digital terrain models (DTM) of Pagham Harbour entrance were produced, covering the period from 27/01/2015 to 03/03/2017. A Geographical Information System (GIS) analysis was then conducted to determine the rate of volume change across the harbour entrance, within pre-defined box cells labelled A-J. Cell A was located furthest updrift, while cells D and E were located over the inlet entrance and cell J was located furthest downdrift of the spit. A wave climate analysis was carried out using wave data from Rustington and Bracklesham Bay wave buoys, to examine variation in significant wave height (H_s), peak wave period (T_p) and wave direction between the winters of 2013/2014 and 2015/2016. Inshore wave energy fluxes and littoral drift rates were also determined over this study period. The crest behaviour observed along Church Norton spit was then modelled using a single cell model, driven by this wave data and the updated littoral drift rates, to determine the effect of overtopping and overwashing on the crest elevation under the given conditions.

The GIS analysis showed that the detached spit migrated downdrift and fused to the shoreline in front of Pagham, while the relic spit continued to recede in a south-westerly direction and showed no evidence of reforming. A decreasing trend was observed in the total volume above -3 m ODN in cells E, F and G while progradation was shown across cells H, I and J, reflecting the migration of the detached spit alongshore. On further division of the cells, based on volumes above and below 0 m ODN, it was clear that most of the volume changes observed in cells H, I and J occurred below 0 m ODN. In the period leading up to the breach, a reduction was also shown in the total volumes for spit sub-cells F and G. The mean values obtained for wave direction, H_s and T_p were all relatively similar. However, the maximum T_p in winter 2013/2014 was notably higher than in winter 2015/2016, with values of 28.6 s and 18.2 s respectively. Comparing the mean inshore wave energy flux between these two winters, the energy flux was shown to be 35.7 % higher in winter 2013/2014 compared to 2015/2016. Two clear peaks in littoral drift were also shown, corresponding to these two winter periods, yet the total annual drift volume has decreased since 2014.

The model results indicated that the Church Norton spit crest lowered through positive feedback loops involving overtopping and overwashing events. The intense storm activity observed in winter 2013/2014 appeared to act as a trigger to the progressive breakdown of a central section of the spit, resulting in overtopping events occurring during summer storm events following winter 2013/2014. The pre-conditioning of this barrier reduced the resilience of the spit by increasing the frequency of overtopping due to the lower energy requirement to overtop the lowered crest. The barrier was then unable to recover due to a limited sediment supply and decreasing annual littoral drift rates after 2014. Consequently, by the start of winter 2015/2016, the elevation of the spit crest had been lowered to such a point that it was left in an increasingly vulnerable position to future storm activity.

Contents

List of Figures

List of Tables

Abbreviations

ABPmer	Associated British Ports Marine Environmental Research
ASMITA	Aggregated Scale Morphological Interaction between a Tidal basin and the Adjacent coast
BODC	British Oceanographic Data Centre
CCO	Channel Coastal Observatory
dGPS	Differential Geographical Positioning System
DTM	Digital Terrain Model
GIS	Geographical Information Systems
GPS	Geographical Positioning Systems
LiDAR	Light Detection and Ranging
LsXs	Longshore to cross-shore ratio
MCZ	Marine Conservation Zone
MHWN	Mean High Water Neaps
MHWS	Mean High Water Springs
MLWN	Mean Low Water Neaps
MLWS	Mean Low Water Springs
ODN	Ordnance Datum
RPM	Revolutions per minute
RTK	Real Time Kinematic
SPA	Special Protected Area
SSSI	Site of Specific Scientific Interest
UK	United Kingdom

Symbols

A_s	Overtopping discharge
C_g	Wave group celerity (m/s)
D_{50}	Mean grain size (mm)
F	Wave energy flux (J/ms)
g	Gravitational acceleration (m/s^2)
H_s	Significant wave height (m)
K_0	Overtopping transport coefficient
s	Bed slope
T_p	Peak wave period (s)
ρ_w	Density of water (kg/m^3)
ϕ	Phi

1. Introduction

1.1. Motivation for this study

The entrance to Pagham Harbour is a highly dynamic area and since the first reliable documentation of the harbour entrance in 1587, the inlet has shown remarkable changes in both size and position, in response to both natural and anthropogenic factors (Scott and Townend, 2017). However, particularly over the past 10 years, the morphological changes observed across the harbour entrance have been rapid and extensive, highlighting the key challenges and difficulties faced in managing such a dynamic section of coastline.

Despite the various attempts over the past 10 years to use training walls and other hard engineered structures to fix the shoreline morphology of the harbour entrance and manage the behaviour of the spit-delta system, success has been limited. The rapid geomorphological changes recently observed at the entrance to Pagham Harbour have important implications, not only to accessing the harbour but also on the shingle supply to Pagham beach frontage. Properties located in the area downdrift of the inlet have been under increasing threat by coastal erosion (Scott and Townend, 2017). Further to this, the site is also of considerable ecological value, accommodating both nationally and internationally protected habitats and species. The site hosts designations as a Ramsar site, a Special Protection Area (SPA), a Site of Specific Scientific Interest (SSSI) and Marine Conservation Zone (MCZ) (Scott and Townend, 2017).

1.2. Study site

Pagham Harbour, located to the east of Selsey Bill on the south coast of the UK (Figure 1), is a small ebb-dominant tidal inlet characterised with a mixed shingle and sand foreshore (Barcock and Collins, 1991). The study area is exposed to wave action from the south-eastern, south-western and southern directions due to the south-west to north-east orientation of the coastline (Barcock and Collins, 1991). Although the headland of Selsey Bill offers some sheltering, this stretch of coastline is subjected to both locally generated storm waves and swells from the Atlantic (Barcock and Collins, 1991). The harbour entrance can be characterised by a maximum significant wave height (H_s) of 3.94 m (HR Wallingford, 1995), as well as spring and neap tidal ranges of 4.9 m and 2.7 m respectively (Barcock and Collins, 1991). To the west of Pagham Harbour, there is a divergence in the littoral drift feed from offshore, marking a littoral sediment cell boundary formed by the protruding headland of Selsey Bill (Bray *et al.*, 1995). Pagham Harbour is also a local RSPB nature reserve.

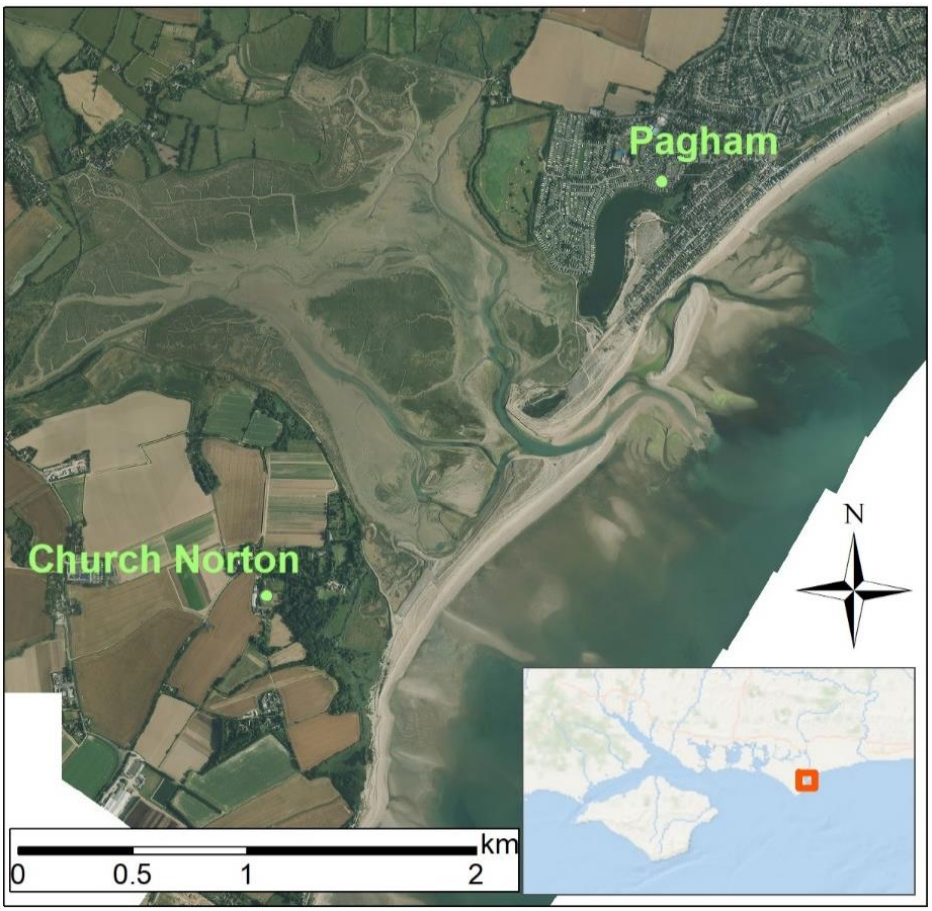

Figure 1-Location of Pagham Harbour entrance, along the central southern coast of the UK. Aerial photography of harbour entrance sourced from CCO.

1.3. Aims and objectives

The overall aims of this study are to determine how Pagham Harbour entrance and the spit system have evolved following the breach of Church Norton spit in spring 2016 and to identify the cause(s) of the breach.

To address the aims of this study, the three main objectives are:

1- To examine the nearshore water level and wave climate, both prior to, and post the breach in 2016, to identify any storm activity before the breach.
2- To assess the rate of volume change of sediment across Pagham Harbour entrance, before and after the breach.
3- To compare the volume changes observed against updrift and downdrift beach profile volumes, before and after the breach, in CoastalTools.

1.4. Hypotheses

The hypotheses to be tested in this study are:

1- The breach along Church Norton spit in spring 2016, was initiated through the lowering of the crest by storm action and developed into a full breach through tidal action.
2- The southern spit is reforming post breach and the relic Church Norton spit is migrating downdrift.

1.5. Literature review

A review of the relevant literature for this study is presented in the following section. The literature reviewed firstly explores gravel barrier systems, providing an overview of the nomenclature and environmental forcing. It will then draw together the literature covering the various aspects of tidal inlet systems including morphology, stability and bypassing mechanisms, with a focus on ebb-tidal deltas. Literature on littoral drift is then covered, before finally exploring the historic morphological behaviour shown at Pagham Harbour entrance and other recent studies undertaken on the harbour entrance.

1.5.1. Gravel barrier systems

Following the Udden-Wentworth scale for grain size classification (Wentworth, 1922), a mean grain diameter of 2 to 256 mm (or -1 ϕ to -8 ϕ) is characteristic of gravel and representative of a coarse-grained beach. While for a fine-grained beach, characterised by sand, the mean grain size is defined as 63 µm to 2 mm (or 4 ϕ to -1 ϕ). However, particle size distribution can vary spatially cross-shore and along the coast and is dependent on the local sediment supply (Stripling *et al.,* 2008), therefore

beaches can be further categorised as mixed (sand and gravel). Particle grain size also governs the natural beach profile. Steeper beach slope angles can be maintained in coarser-grained sediment, due to a greater angle of repose (Kirk, 1980) and this gives rise to the reflective nature of a gravel beach shoreface (Nicholls, 1985; Pye, 2001). Additionally, gravel beaches have a higher permeability, enabling further energy dissipation of incoming waves (Anthony, 2008). In comparison, fine-grained beaches are dissipative in nature, displaying a milder beach slope angle and lower permeability. A typical cross-sectional profile of a gravel barrier incorporates distinct features such as a crest, from which landward and seaward slopes can be distinguished, berm(s) on the beach face and a steep foreshore and back slope (Figure 2).

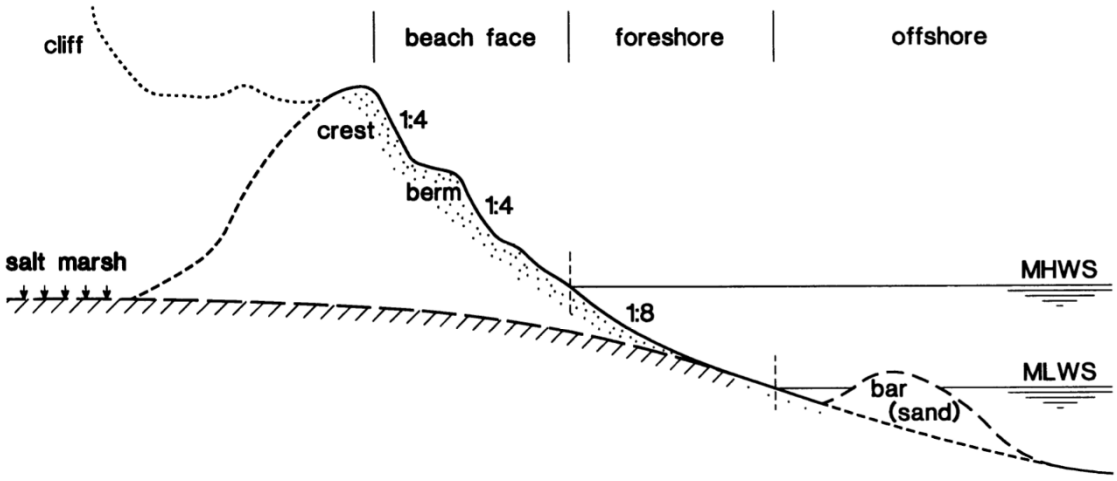

Figure 2- Schematic cross-sectional profile of a coarse-grained barrier beach (Van Rijn and Sutherland, 2011).

Barrier beaches can be further categorised as 'drift aligned' or 'swash aligned', dependant on the orientation of the barrier beach to the dominant wave action. 'Drift aligned' beaches are orientated at an angle to the predominant direction of incident waves and therefore governed by the longshore transport of sediment. Whereas the orientation of 'swash aligned' beaches are perpendicular to the predominant incident wave direction (Masselink and Russell, 2013).

As discussed previously, shingle barriers and beaches are hydraulically efficient and important permeable natural defences, offering protection against wave attack to low lying regions located leeward, by dissipating wave energy (Bradbury and Powell, 1992). They are predominantly located on wave dominated coastlines at mid-high latitudes (McCall *et al.,* 2013) and the evolution of these coarser grained barriers is predominantly influenced by the availability of sediment rather than fluctuations in sea level (Stripling *et al.,* 2008). For gravel beaches, wave action is suggested to form the main driver of sediment transport (Pye, 2001) and therefore form a primary control on the

morphology (Wright and Short, 1984). Compared to sandy beaches, where the movement of material occurs predominantly through suspension and tidal currents, the movement of shingle occurs largely as bedload transport (Velegrakis, 1994). During the swash phase on gravel beaches, grain particles are moved up the beach by the strong uprush, in the same direction as the incoming waves. During the weaker backwash phase, the grain particles move seaward by gravity and the retreating wave. The backwash phase is weaker as a result of percolation into the gravel barrier. This creates a 'saw-tooth' style of grain movement along the beach and at a larger scale results in the longshore sediment transport (Van Rijn and Sutherland, 2011).

1.5.2. Morphology of tidal inlet systems

The morphology of a tidal inlet incorporates many components, including ebb and flood tidal deltas, also referred to as seaward and landward shoals respectively. Hayes (1969) defined an ebb-tidal delta as the accumulation of sediment on the seaward side of a tidal inlet. Ebb-tidal deltas host a main ebb channel, which in turn may be flanked by channel-margin linear bars on a broad swash platform, generated through the interaction between currents generated by waves and tidal currents. The presence of marginal flood channels has been suggested to prevent the attachment of these swash bars to the nearby barrier beach. An additional morphological component of an ebb-tidal delta is the terminal lobe, which is situated at the seaward end of the main ebb channel and where water depth increases rapidly seaward (Hayes, 1980) (Figure 3). Flood-tidal deltas in turn, host a series of flood channels which bifurcate across the delta and a flood ramp (Hayes, 1980).

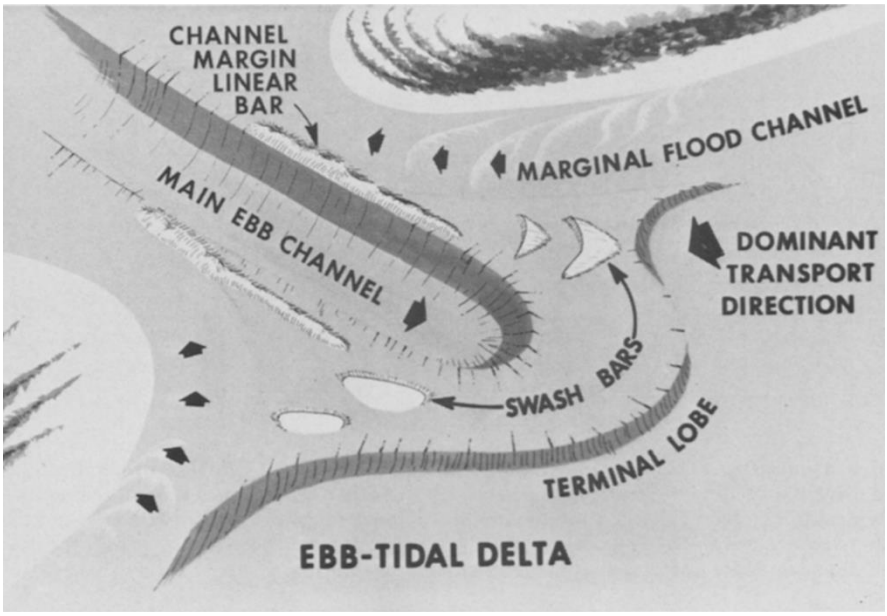

Figure 3- Morphology of an ebb tidal delta. The direction of tidal currents is indicated by the arrows (Hayes, 1980).

The dynamic nature of tidal inlets is closely linked to the inlet's stability, where the stability in turn is controlled by factors including the asymmetry in ebb and flood tide duration, the tidal prism of the harbour, littoral drift and freshwater discharge (Gao and Collin, 1994). The presence of an ebb tidal delta can wield a considerable morphodynamical influence on the nearby shorelines (FitzGerald, 1988), and provide an important component in local sediment budgets (Hicks and Hume, 1996). Additionally, sediment updrift of an inlet entrance can be transferred to the downdrift of the inlet entrance through a mechanism known as ebb delta bypassing, therefore facilitating longshore sediment transport (Burningham and French, 2006). Previous studies have shown the method of sediment bypassing to vary, depending on the ratio between the littoral drift rates and the maximum spring tide discharge through the inlet. A low ratio suggests sediment bypassing occurring via shoal migration or channel transport, while a high ratio indicates bypassing around the edge of the ebb tidal delta driven by wave action (Brunn and Gerritsen, 1959).

There are several different mechanisms in which sediment can bypass an inlet, which vary depending on the stability of the inlet. Firstly, for an inlet with a stable main ebb channel, bypassing can occur through the migration of bars in a landward direction before merging to the shoreline, downdrift of the inlet. The bars described here are formed through merging together and stacking of swash bars present on the ebb delta swash platform (FitzGerald *et al.,* 2000).

A second bypassing mechanism shown in tidal inlets that have a stable throat position, yet display a cyclical behaviour in the migration of the main ebb channel downdrift, can occur through ebb-tidal delta breaching. The accumulation of sediment updrift of the ebb-tidal delta, formed because of a preferential direction in alongshore transport, can consequently lead to the deflection of the main ebb channel downdrift. If this deflection is large enough, this can reduce the hydraulic efficiency of the main channel and the ebb flow will find an alternative path through the ebb-tidal delta causing ebb-tidal delta breaching to occur. The process of breaching allows a large volume of sediment bypass the inlet mouth and the old inlet channel infills through the deposition of sediment by currents, generated by waves and the tide. The rate at which this breaching takes place can increase substantially during a storm event (FitzGerald *et al.,* 2000). In a previous study focusing on the Debden Estuary in Suffolk, a comparability was noted between the ebb delta bypassing of a gravel inlet and the 'ebb delta breaching' model developed by FitzGerald (1988).

A third mechanism in which bypassing can take place is via the migration of an inlet and spit breaching. As sediment is transported alongshore, it can be deposited in the inlet and consequently reduces the flow through this inlet. The effect of this constriction leads to higher current velocities and increased scouring. A dominance in the longshore transport direction causes the migration of the

inlet and during this, a trail of curved beach ridges is left behind along the updrift spit. Further to this, there can be a reduction in the tidal range of the harbour, due to the longer inlet channel length created as the inlet migrated. This results in an increased frictional component, resisting tidal flow and the resulting differences in the tidal range and phase, seaward and landward of the spit, can increase the potential for a breach to occur (FitzGerald *et al.,* 2000).

1.5.3. Littoral Drift

Littoral drift is an important component to consider for this study. Firstly, it acts as a pathway to deliver a supply sediment along the coast from updrift sources (Cope, 2004), which in turn can exert a considerable influence on the volume of barrier beaches and spits and the stability of tidal inlets. Harbours and tidal inlets form major barriers to littoral drift (Bray *et al.,* 1995) and hence the updrift accumulation of sediment in response to high littoral drift rates, can result in the elongation of barrier beaches and spit development (Aubrey and Gaines, 1982). An episodic, progressive reduction or generally low littoral drift rates however, can have detrimental impacts on the downdrift coastline, leading to sediment depletion (Bray *et al,* 1995) and areas of erosion. In cases where people and properties are at risk of coastal erosion and flooding, there is therefore a requirement for forward-thinking coastal management strategies and engineering schemes to be implemented to help reduce these risks (Cooper and Pontee, 2006). The direction of littoral drift can also vary in response to changes in the wave direction (Stripling *et al*., 2008), resulting from changes to the wider wave climate or through localised wave refraction (Bray *et al.,* 1995).

1.5.4. Historical morphological behaviour of Pagham Harbour entrance

Using the earliest reliable chart, dated 1587, the harbour entrance was shown to host two shingle spits. The southern spit prograded a distance of 90 m in a north-easterly direction by 1724 and an additional 900 m by 1874 (Scott and Townend, 2017). In 1876 there was a deliberate closure of the inlet, lasting for 34 years and resulting in seaward extension of Pagham Beach due to the onshore transport of eroded ebb delta material. Following the storm-induced breach which occurred to the southern spit in 1910, the southern spit once again prograded a distance of approximately 700 m along the coast towards Pagham Beach (Scott and Townend, 2017). Sheet piling was introduced in 1944, to help stabilise the inlet. However, in the period over the 1950s and 1960s, a storm-induced breach occurred in 1955 and the inlet was shown to widen and migrate in a northly direction, approximately 900 m along the coast (Scott and Townend, 2017).

1.5.5. Morphological behaviour of Pagham Harbour entrance over the past 15 years.

The double-spit system characterising Pagham Harbour entrance has shown considerable morphological changes over the past decade. In 2003, the southern spit began to prograde in a north-east direction along the coastline, reflecting a switch in behaviour from ebb delta bypassing to spit progradation. The switch to spit progradation observed, forced the tidal inlet to migrate in a north-east direction, leading to groyne damage and accelerated local erosion along Pagham frontage (Scott and Townend, 2017). Until 2004 interventions were also carried out in the form of shingle recycling, initially by the National Rivers Authority (NRA) but later by the Environment Agency. The intervention works involved building up the shingle ridge of Church Norton spit following storms, by placing 15,000 m^3/year of shingle sourced from the ebb delta (Scott and Townend, 2017). From 2003 to 2015, the southern spit continued to prograde, however, at the start of 2016 there was evidence of roll back occurring within a central section of the southern spit. By February, this central section had shown considerable lowering over a 90-100m long section, allowing for high water exchange to occur. The breach then widened and increased in depth, during a series of storm events in March 2016 (Scott and Townend, 2017).

1.5.6. Previous studies on Pagham Harbour

A previous study investigating the causes, patterns and rates of beach erosion along Pagham frontage was carried out by Barcock and Collins (1991). The results from this study showed a small area along the frontage with a rapidly decreasing erosion rate, bound by areas of accretion. The observed area of erosion was suggested to be due to a localised drift reversal, in turn caused by wave refraction over the ebb tidal delta. Fluctuating periods of erosion and accretion, shown to the east of the inlet channel were thought to be a result of the ebb delta migrating and welding to the down drift shoreline.

More recent studies, focusing on the period over the past 15 years, found that the volume of sediment contained within the Church Norton spit, that fronts Pagham Harbour, had increased. The rate of this observed increase was found to be in line with estimates of littoral drift, indicating that limited bypassing occurred over this period (Townend, 2015). Recent estimates of littoral drift along this section of coastline indicated peak rates of 40,000 m^3/year and normal littoral drift rates of between 15-25,000 m^3/year (Townend, 2015), which is in broad agreement with previous estimates of littoral drift rates by Barcock and Collins (1991).

Other studies focusing on the spit-delta migration at the entrance to Pagham harbour, have highlighted a close coupling between the supra-tidal spit and the ebb delta and the prograding spit was shown to follow the migration of the ebb delta (Townend, 2015). Additionally, the temporal and spatial patterns of erosion and accretion were shown to be closely related to the varying position of the inlet channel and spit system (Royal Haskoning, 2009). Other studies found that large shore-normal spurs, migrating in a north-easterly direction, periodically supplied Pagham Harbour frontage with shingle (Barcock and Collins, 1991). Although submerged bars located on the ebb tidal delta, were shown to behave as a barrier and disrupt sediment transport (Royal Haskoning, 2009). In addition to the previous morphological studies conducted on Pagham Harbour entrance, a study by Cundy *et al.* (2002) was conducted to investigate the sedimentary response of the harbour itself, to the breach of the barrier in 1910, using stratigraphic sediment cores and radiometric dating techniques.

Figure 4- Photographs of Pagham Harbour entrance taken during the site visit in May 2017: (A) A view along the stoss side Church Norton spit in a south-westerly direction towards Selsey Bill; (B) A view of the lee side of Church Norton spit, from a northern direction across the inlet channel on Pagham spit; (C) A view across Pagham Harbour entrance, showing private properties to the north and a body of sediment newly adjoined to the shoreline to the south. All photos kindly provided by Professor Ian Townend.

2. Methodology

The following section presents the methodology required to achieve the objectives defined for this thesis and covers the three key stages of this study: GIS analysis; Wave climate analysis and Overtopping-overwash spit modelling.

2.1. Data collection

2.1.1. Sediment sample collection

A visit to the study site was conducted on 03/05/2017, with the primary purpose to obtain sediment samples down to the low tide mark and gain a better understanding of the layout of Pagham Harbour entrance (Figure 4). A total of 7 sediment samples were collected and the global positioning system (GPS) waypoints recorded for each, using a Garmin GPS handset. These samples were spatially distributed over the entire study site, including the crest and spit flanks of both Pagham spit and Church Norton spit, two locations on the ebb delta and one sample at the low tide mark of Church Norton spit. This was to ensure samples covered the cross-shore and alongshore variation of the study site.

2.1.2. Sediment sample analysis

Samples were rinsed thoroughly with freshwater, transferred quantitively to an aluminium tray and then placed into an oven at 50 °C to dry. Once dry the samples were quantitively transferred to an Endecotts Octagon 200 sieve shaker with a graded sieve mesh stack and were shaken at 2000 RPM for 10 minutes. Following the shaking stage, sediment retained on each mesh was weighed and GRADISTAT 4.0 (Blott and Pye, 2001) was used to determine the sediment grain statistics.

2.1.3. Summary of datasets

A summary of all the datasets used are shown in Table 1.

Source	Data/survey type	Detail
Channel Coastal Observatory (CCO)	Topographic baseline	Pre-breach survey dates: - 27/01/2015 - 02/06/2015 - 04/09/2015 - 29/01/2016 Post breach survey dates: - 13/04/2016

		- 24/06/2016 - 07/09/2016 - 03/03/2017
	Topographic profiles	All profile surveys available between 01/01/2012 and 31/05/2017. Survey unit: 4dSU22 - P4d01382 - P4d01377 - P4d01371 - P4d01364 - P4d01359 Survey unit: 4dSU23 - P4d01410 - P4d01405 - P4d01403 - P4d01398A - P4d01397 - P4d01391 - P4d01387 Survey unit: 4dSU24 - P4d01423 - P4d01458
	Swath bathymetry	- 06/06/2016 - 1 m resolution - Conducted using a Kongsberg EM3002D
	Light Detection and Ranging (LiDAR)	- 04/03/2014 - 30/03/2014 - 1m gridded resolution
	Wave	Wave data including H_s, T_p, maximum wave height and wave direction. Rustington wave buoy - (50˚ 44.06’ N, 000 ˚ 29.64’ W)

		- Data from 01/01/2012- 31/05/2017 Bracklesham wave buoy - (50˚ 43.36’ N, 000˚ 50.33’ W) - Data for 01/01/2012- 31/05/2017
British Oceanographic Data Centre (BODC)	Water levels	- Portsmouth tide gauge - (50° 48' 09.2" N, 01° 06' 42.3" W) - 01/01/2012 to 31/05/2017 - 15 minute sampling intervals
Associated British Ports Marine Environmental Research (ABPmer)	Inlet channel depth measurements	- 05/03/2015 and 14/03/2015 - 4 transects
Site fieldwork	Sediment grain size	-

Table 1-A summary of the datasets used in this study.

2.2. GIS analysis

The following section describes the initial DTM set-up and GIS tool application for each GIS tool analysis. All GIS analysis were carried out in the ArcMap suite of ArcGIS 10.4.

2.2.1. Digital Terrain Model set-up

A total of eight DTMs were produced in ArcMap, corresponding to the eight most recent topographic baseline surveys carried out at the study site, from 27/01/2015 to 03/03/2017. To create these DTMs, topographic baseline data, LiDAR data, swath bathymetry data and channel depth data were combined.

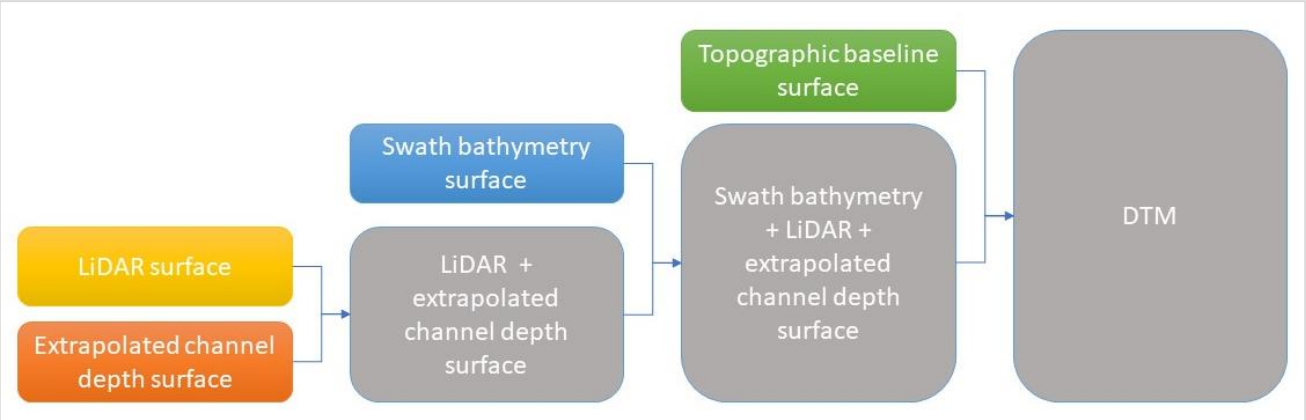

Figure 5- A flowchart summarising the mosaic sequence followed to create each digital terrain model.

The first stage used the 'Mosaic to new raster' tool to mosaic together swath bathymetry data tiles for the most recent swath bathymetry survey conducted offshore of Pagham on 06/06/2016. This step was then repeated using LiDAR data from 2014. To obtain a sufficient spatial LiDAR coverage for Pagham Harbour and the surrounding coastline, LiDAR survey data from 04/03/2014 and 30/04/2014 were mosaiced together. The LiDAR data from 04/03/2014 provided spatial coverage of the immediate surrounding coastline, while the LiDAR data from 30/04/2014 provided complete coverage of Pagham Harbour. For the topographic baseline data, a mask was created for the wider Pagham Harbour region and the point elevation data was then extrapolated over this mask region, using the 'Topo to raster' tool. The "Extract by mask" tool was then used to clip this extrapolated topographic surface to the area covered by the survey. Following this, the depth measurement data obtained from 4 transects covering a 150 m wide section of the main inlet channel, provided by ABPmer, was extrapolated over the harbour entrance area using the 'Topo to raster' tool. These depth measurements were collected on 05/03/2015 and 14/03/2015 using a Real Time Kinematic (RTK) differential Global Positioning System (dGPS) (ABPmer, 2015).

To combine the clipped topographic baseline surface, LiDAR, swath bathymetry and the extrapolated channel surface, the 'Mosaic to new raster' tool was used in sequence (Figure 5). Firstly, the LiDAR surface was mosaiced to the extrapolated channel surface to create a new surface. By specifying the mosaic operator as 'FIRST', this ensured that the cell output for clashing cells was the value of the first input raster, which in this first case was the LiDAR surface. This step was repeated to combine this newly made LiDAR and channel surface and the swath bathymetry surface. Again, the mosaic operator was specified as 'FIRST', to ensure the value of the new cell output for any clashing input cells was the value of that cell in the swath bathymetry input raster. This process was repeated a third

time to mosaic together the clipped topographic baseline surfaces and the combined swath bathymetry, LiDAR and channel surface to create the final digital terrain models.

In some digital terrain models, a ghost spit was visible underneath the topographic survey surface, due to the position of Church Norton spit in the 2014 LiDAR data. To remove this a LiDAR mask was defined for each individual survey affected, and the "Erase" tool was used to remove this mask area from the wider Pagham Harbour region mask. The "Extract by mask" tool was then used to crop the 'ghost' region from the 2014 LiDAR surface, before then mosaicing each surface again in turn, following the steps described previously. This step was repeated for each DTM that was affected.

2.2.2. Volumetric 'Box' analysis

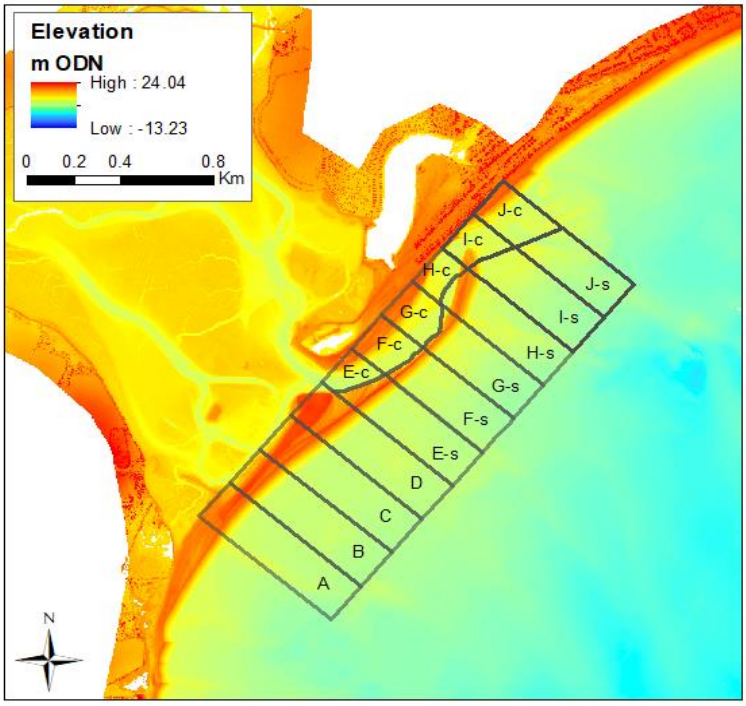

Figure 6- Location of cells A to J, including channel and spit sub-cells, used in the volume analysis.

The area of interest was divided into 10, 200 m alongshore wide cells labelled A to J, identical to those used in the previous study of this site by ABPmer. In a cross-shore direction, these cells were defined from a line determined landward of any change in the foreshore, to the furthest extent of data seaward. This was generally just below -3 m to ordnance datum (ODN). For survey dates prior to the breach (27/01/2015 to 29/01/2016), cells E to J were further divided into 'channel and landward' and 'spit and seaward' sub-cells, defined by the 0 m ODN contour extracted on the landward side of Church Norton spit (Townend, 2015) (Figure 6).

For each cell and sub-cell, the volume was computed for sediment above specific plane elevations of -3 m, 0 m and +3 m ODN, using the 'Surface volumes (3D Analyst)' tool. For survey dates post-breach (13/04/2016 to 03/03/2017), no sub-cells were defined and sediment volumes were calculated using the same method described previously for the full cells. No sub-cells were defined for the surveys following the breach, as it was no longer appropriate due to the substantial morphological changes that have occurred since the sub-cells were first defined in a previous study by ABPmer. An overview of this volumetric 'box' analysis is shown in Figure 7.

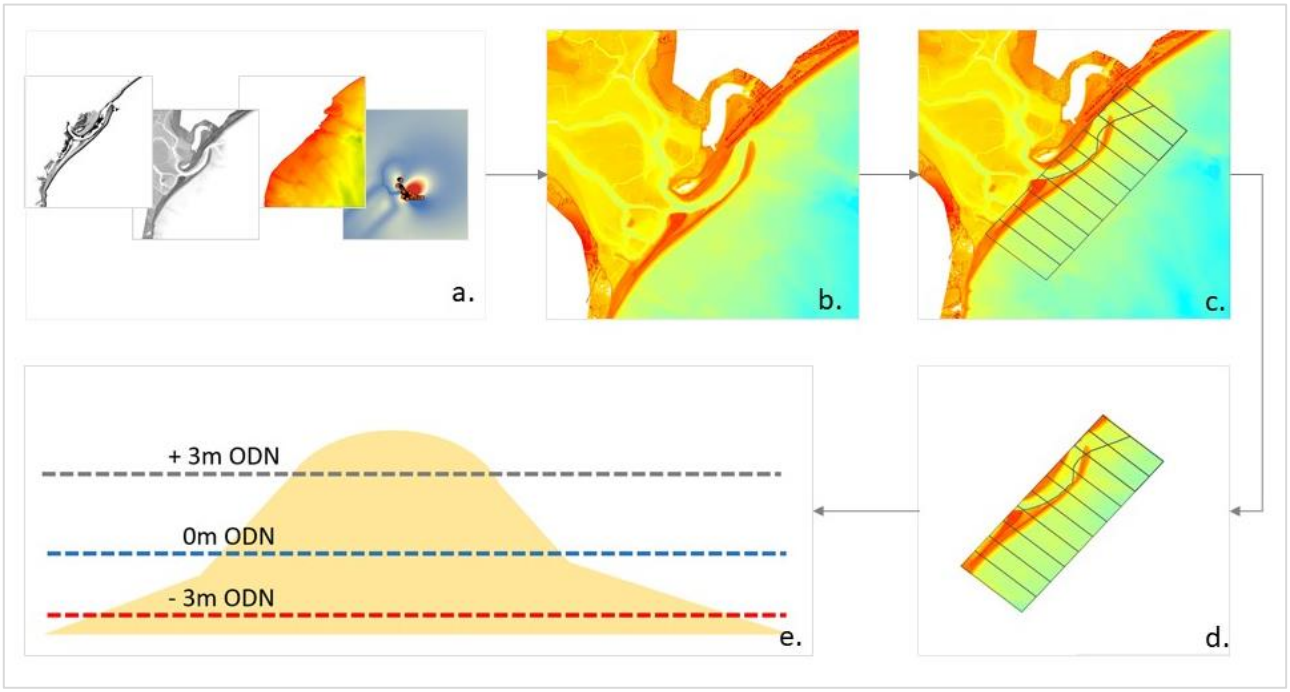

Figure 7- An overview of the volume 'box' analysis method: (a) Combining topographic baseline, LiDAR, swath bathymetry and extrapolated dGPS measurement data; (b) Creation of DTMs; (c) Application of pre-defined cells and sub-cells; (d) Clip DTMs to cells and sub-cells; (e) Extracting sediment volumes above set elevation planes.

2.2.3. Spit-delta contour migration

Using the 'Contour' tool in ArcMap, a base contour at 0m ODN and contours at intervals of 0.5 m ODN, above and below the base contour were obtained. To maintain consistency with a previous Pagham study carried out by ABPmer, elevation contours at +3 m, 0 m and -0.5 m ODN were chosen for analysis. These were extracted by selecting these contour elevations from the attribute table one by one, and using the 'Clip (Analysis)' tool to clip the selected contour.

2.2.4. Spit distal point migration

The distal point of the spit was determined by eye, using the 'Identify' tool in ArcMap to obtain the easting and northing position. The 'Measure' tool was then used to measure the distance in metres between the changing position of the distal point across the different surveys.

2.3. CoastalTools

2.3.1. Wave climate and water level set-up

Wave climate data for the Rustington wave buoy, for the period from 01/01/2012 to 31/05/2017, was obtained from CCO. Due to a notable gap in the wave climate record from Rustington wave buoy between 11/02/2016 and 01/03/2016, data from Bracklesham Bay wave buoy was used to infill this period. To check that this was appropriate, a linear regression analysis of significant wave height (Hs) over July 2016 was conducted between the two wave buoy datasets. This returned a coefficient of determination (R^2) value of 0.94, shown in Figure 8.

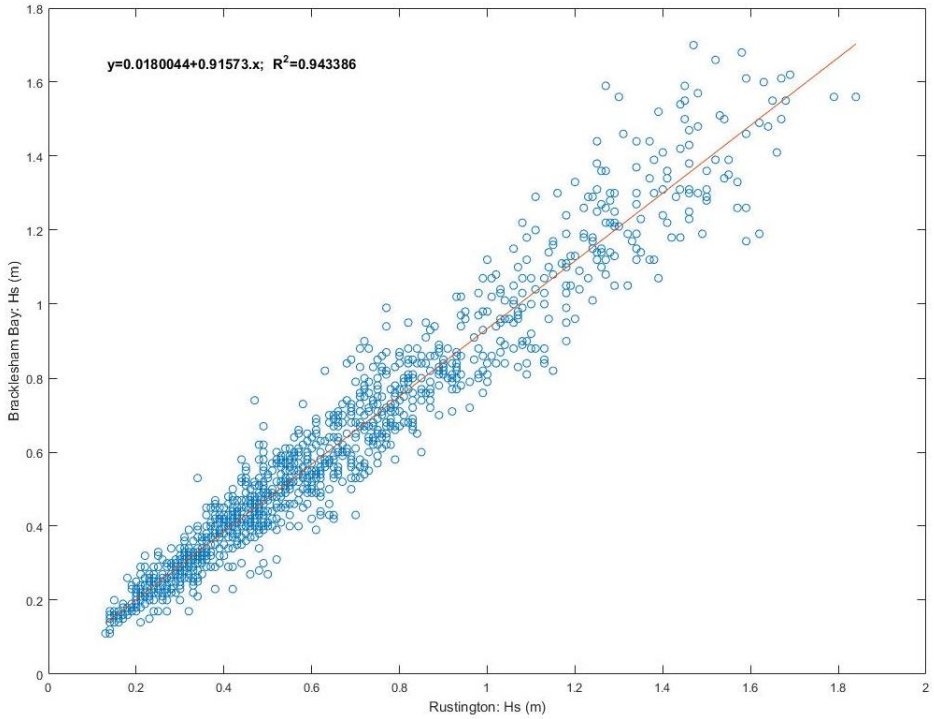

Figure 8- Linear regression of Hs between Rustington and Bracklesham Bay wave buoys for July 2016.

Tide data was obtained for Portsmouth from the British Oceanographic Data Centre (BODC). This data was then adjusted for the secondary port, Selsey Bill, using tidal height differences provided in the Admiral Tide Tables to determine a ratio 'r'. The tide level for Portsmouth was then multiplied by 'r', to obtain an adjusted water level record for Selsey Bill.

$$r = \frac{MHWS_{Sel} - MLWS_{Sel}}{MHWS_{Ports} - MLWS_{Ports}} \quad (1)$$

Equation 1: Formula used to adjust water level data sourced for Portsmouth (Primary port) to Selsey Bill (Secondary port).

2.3.2. Overtopping model

An overtopping volume for the shingle spit was estimated using the formula for overtopping proposed by Owen (1980), by defining a structure in the model that represented an appropriate beach crest and slope. The model also took into consideration factors including the beach roughness and berm width, although in this study no berm was defined. The level of the crest and toe were defined relative to ordnance datum, the same datum defining the water level used in the model (Townend, 2016). The structure parameters defined are shown in Table 2.

Structure Parameters	Value
Crest level (m)	5
Crest width (m)	1
Upper slope (1:m)	5
Berm level (m)	0
Berm Width (m)	0
Lower slope (1:m)	5
Toe level (m)	-2
Wall roughness	0.6

Table 2- Structural parameters defined in overtopping model.

2.3.3. Longshore drift model

Estimates of littoral drift along this section of coastline were calculated using the Longshore Drift model, which used the Damgaard and Soulsby formula for longshore sediment transport along shingle beaches (Soulsby, 1997). In comparison to the original CERC formula for longshore transport, the Damgaard and Solusby formula takes into consideration the slope of the beach, grain size and wave period (Soulsby, 1997). The inputs for this model were the inshore wave parameters and the site parameters defined in Table 3.

Site Parameters	Value
Bed level offshore (m OD)	-10
Bed level at beach toe (m OD)	-3
Angle of shoreline (deg TN)	48
Friction coefficient	1
Drift coefficient (kc)	$6x10^{-4}$
Nearshore bed slope (1:m)	100
Bed slope (1:m)	20
Grain size (d50) (m)	0.015
High water level (m OD)	3
Low water level (m OD)	-2

Table 3- Site parameters defined for longshore drift and wave energy models.

2.3.4. Wave energy model

Using the adjusted wave data for Rustington wave buoy, the wave energy model used linear wave theory and plane bed refraction and shoaling to calculate inshore wave parameters. Once calculated, a check was conducted on the inshore wave height to determine any wave breaking, using the water depth and wave period, in addition to the nearshore bed slope defined in the site parameters (Table 3). This model then used linear wave theory to calculate the inshore wave energy flux (J/ms) (Townend, 2016).

$$F = g.\rho_w.\frac{H_s^2}{8}.c_g \quad (2)$$

Equation 2: Calculation of wave energy flux using linear wave theory.

2.1.1. Beach profile volume set up and model

A total of 14 baseline profiles were selected from survey units 4dSU22, 4dSU23 and 4dSU24, to cover the regions both updrift and downdrift of the harbour entrance, in addition to the harbour entrance itself. A volume model was then run in CoastalTools to determine the area per unit metre width under each profile, with a set of x and z boundaries specified for each profile. The z-boundary was kept at a constant value of -2 m ODN, while the limit of the x-boundary varied between different profile lines

and was based on the general location of the shingle crest displayed for each profile line over the timeseries of that profile line. The location of each profile line is shown in Figure 9.

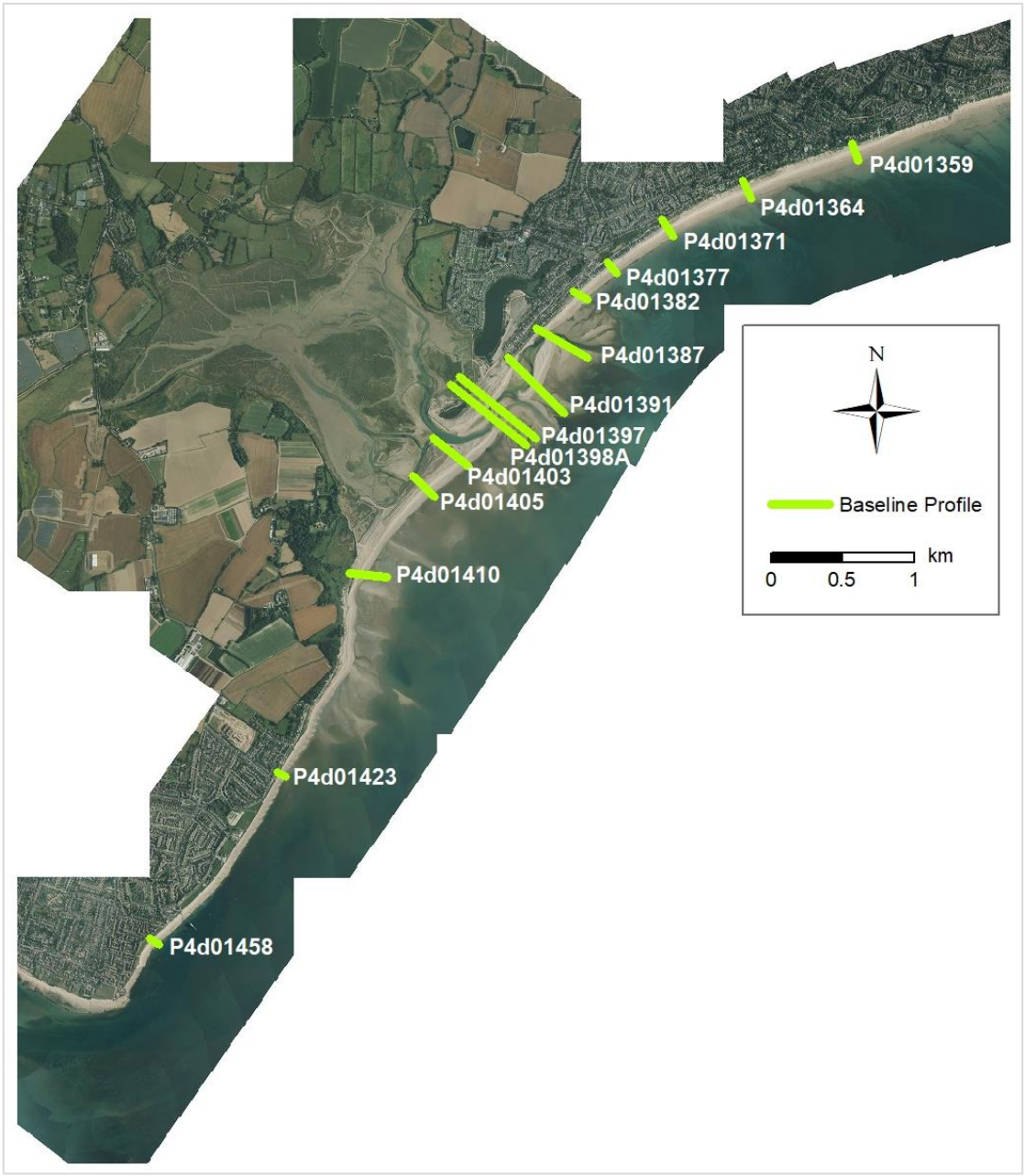

Figure 9- Location of baseline profiles. Aerial photography of harbour entrance sourced from CCO.

2.4. Breach model

2.4.1. Spit overtopping and overwash model

A simple model was used to determine an estimate of overtopping, overwashing and variations in the crest level. This model was run for the period between 01/01/2012 to 31/05/2017 and used the adjusted wave data from the Rustington wave buoy and water level data for Selsey Bill, adjusted from the Portsmouth tide gauge. The rate at which sediment was imported into this model was controlled by the littoral drift rate estimated using the Daamgard and Soulsby (1997) formula for bedload longshore transport on shingle beaches. Based on Soulsby (1997), the overtopping transport coefficient (k_0) used in this model was calculated using the overtopping discharge given by the following equation:

$$As = \frac{k_0.d_{50}.D_s^{-0.6}}{((s-1).g.d_{50})^{1.2}} \quad (3)$$

Equation 3: Overtopping discharge.

The model returned estimates for the overtopping sediment volume, an overwash drift volume and the net surplus volume (Townend, 2016), in addition to variations of the crest levels of the defined element and a downdrift element. If the water level was below the crest of the spit, an overtopping rate was first calculated and then used to determine a volume of sediment removed by overtopping. However, if the water level was above the level of the crest, then an additional drift calculation was performed, taking the water depth above the spit into consideration. The crest elevation and spit volume were updated. If the maximum defined elevation of the spit element was exceeded by the updated crest level, the excess volume above this maximum elevation level was added to the output volume. The final values of model parameters used are summarised in Table 4.

Model properties	
Element width (m)	150
Element length (m)	200
Bed level (m ODN)	-0.5
Initial crest level (m ODN)	5
Max crest level (m ODN)	5
Crest width (m)	20
Spit slope (1:m)	6
Roughness	1
Overtopping transport coefficient	17
Sediment transport formula	Damgaard and Soulsby (1997)

Table 4- Spit overtopping and overwash model parameters.

3. Results

This results from this study are presented in the following section, covering the volumetric changes over the harbour entrance and adjacent coastline, a comparison of the wave climate between the winters of 2013/2014 and 2015/2016, an updated estimate of littoral drift for this length of coastline and model results from the simplified overtopping-overwash model.

3.1. Recent morphological behaviour of Pagham Harbour entrance

3.1.1. Volumetric 'box' analysis

In general, there was a decreasing trend in the total volume above -3 m ODN in cells E, F and G observed, while progradation was shown across cells H, I and J. Between 27/01/2015 and 03/03/2017, the total volume above -3 m ODN in cells E, F and G decreased by 30.3 % from $1.07x10^5$ m^3 to $7.46x10^4$ m^3, 36.7% from $1.22x10^5$ m^3 to $7.72x10^4$ m^3 and 35.4 % from $1.12x10^5$ m^3 to $7.23x10^4$ m^3 respectively. In comparison, the total volume in cell I increased from $3.69x10^4$ m^3 on 27/01/2015 to $8.36x10^4$ m^3 by 03/03/2017, indicating an increase in volume of 126 % in this period. However, it is clear on further subdivision of the total volumes above and below 0 m ODN, that most of these volume changes observed in cells H, I and J occurred below 0 m ODN (Figure 10). For cells A to D, the total volumes above 0 m ODN remained relatively consistent since 2012. In the spit sub-cells F to J, a clear growth in the volume above 0 m ODN was shown (Figure 11), corresponding to the progradation of the spit along the coastline. However, in the period leading up to the breach a reduction in the total spit volumes across sub-cells F and G was shown.

This was further highlighted in Figure 12, showing the normalised total cell volumes. Focusing on the period leading up to and after the breach, the main change was shown to occur above 0 m ODN in cells E to G, indicated by the negative volume change relative to the mean of section starting prior to 2016 (Figure 11). In comparison, cells I and J displayed an increasingly positive volume change above 0 m ODN, indicating the migration of the detached spit along the coastline.

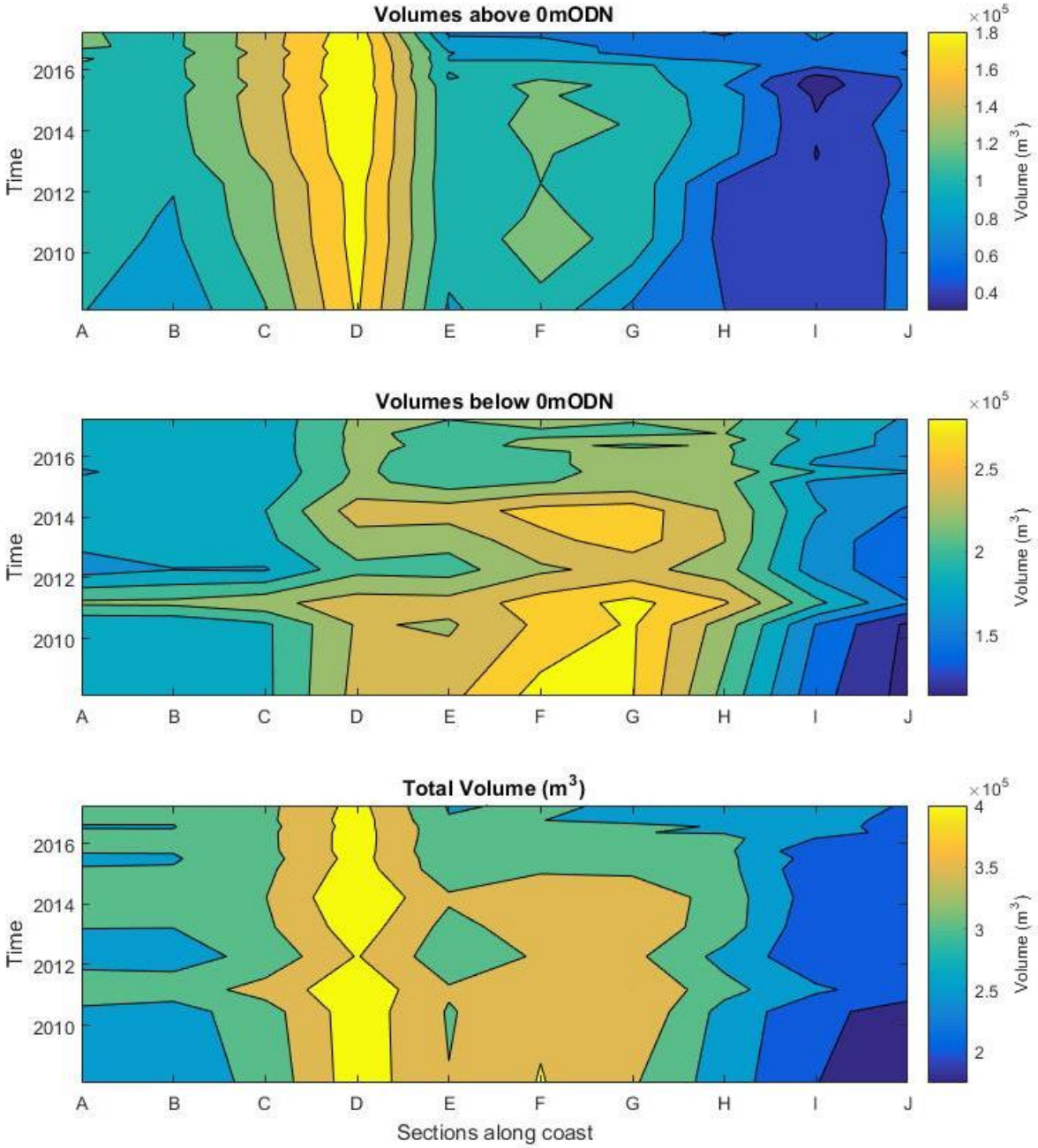

Figure 10- Total sediment volume across cells A to J, between 31/01/2008 and 03/03/2017: (Top) Sediment volume above 0 m ODN; (Middle) Sediment volume below 0 m ODN; (Bottom) Total sediment volume above -3 m ODN.

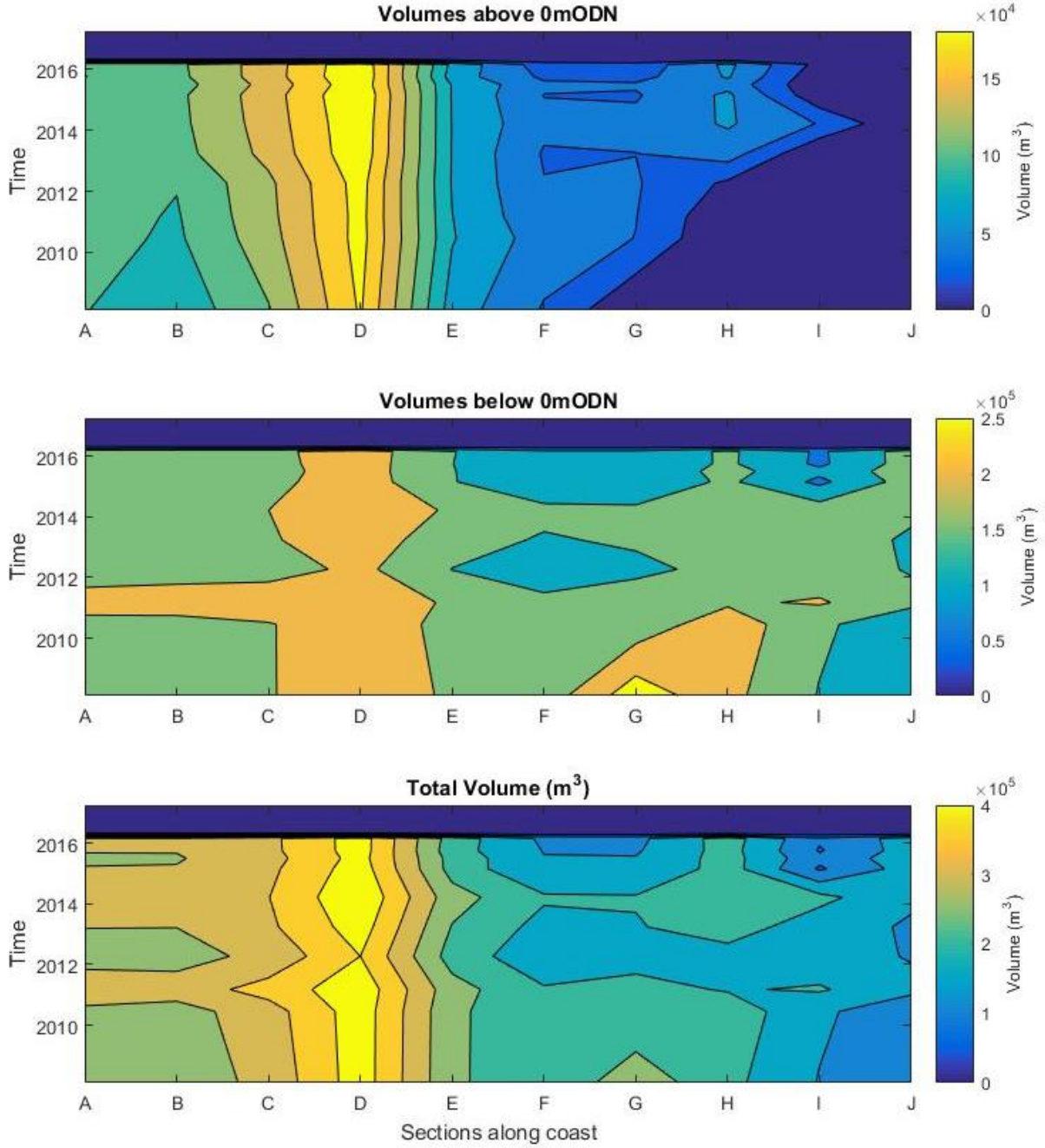

Figure 11- Total sediment volume across cells A to D and spit sub-cells E to J, between 31/01/2008 and 03/03/2017: (Top) Sediment volume above 0 m ODN; (Middle) Sediment volume below 0 m ODN; (Bottom) Total sediment volume above -3 m ODN.

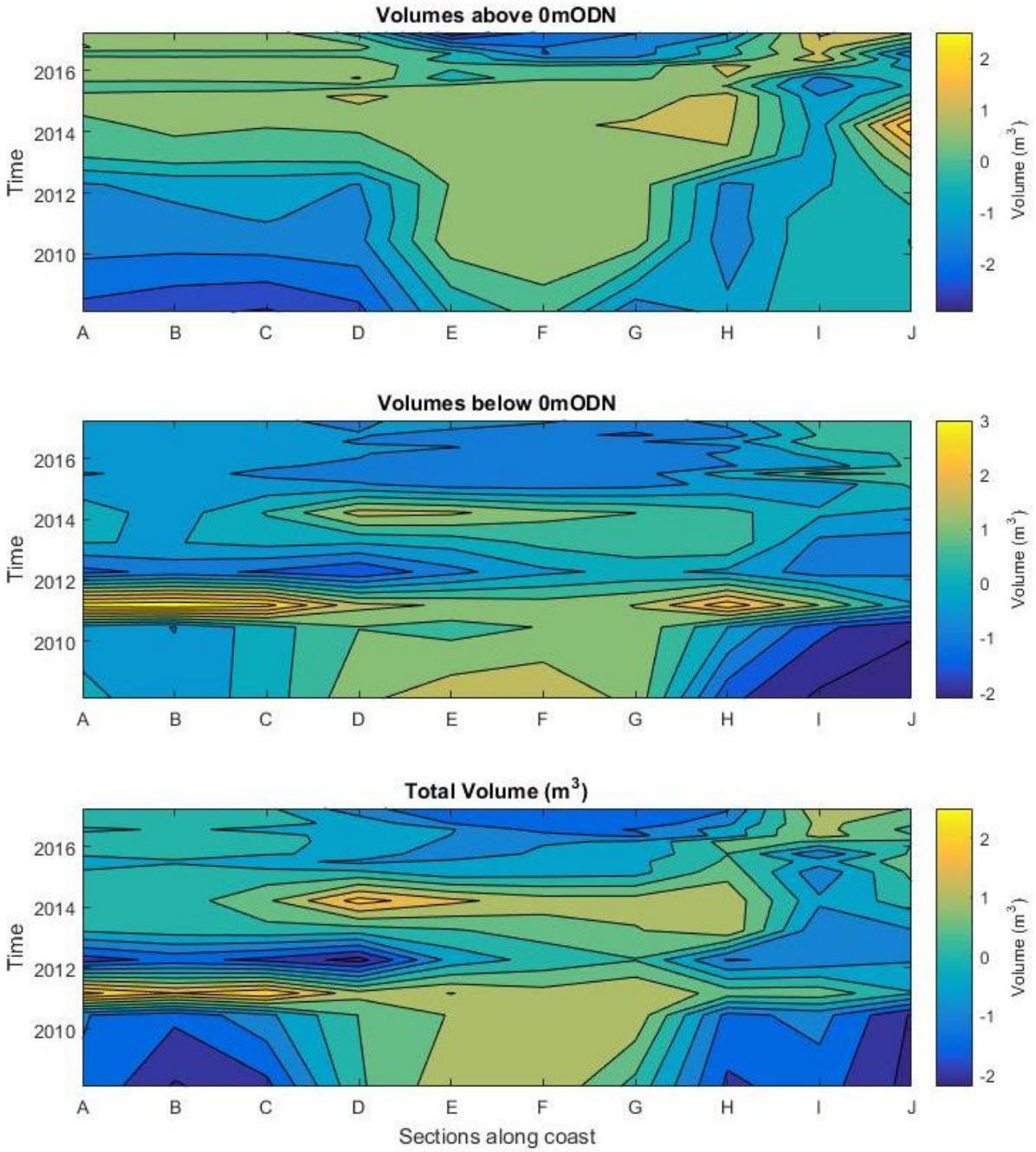

Figure 12- Normalised total sediment volume across cells A to J, between 31/01/2008 and 03/03/2017: (Top) Sediment volume above 0 m ODN; (Middle) Sediment volume below 0 m ODN; (Bottom) Total sediment volume above -3 m ODN.

3.1.2. Spit distal point migration

The position of the distal point for Church Norton spit was tracked from 27/01/2015. The 3 m ODN distal point migrated in a north easterly direction along the coastline. Between 27/01/2015 and 07/09/2016, the northern distal point migrated a total distance of 126.8 m, with the greatest individual migration distance occurring between 04/09/2015 and 29/01/2016 of 89.5 m (Figure 13). Following 07/09/2016, the 3 m ODN distal point fused with the downdrift shoreline.

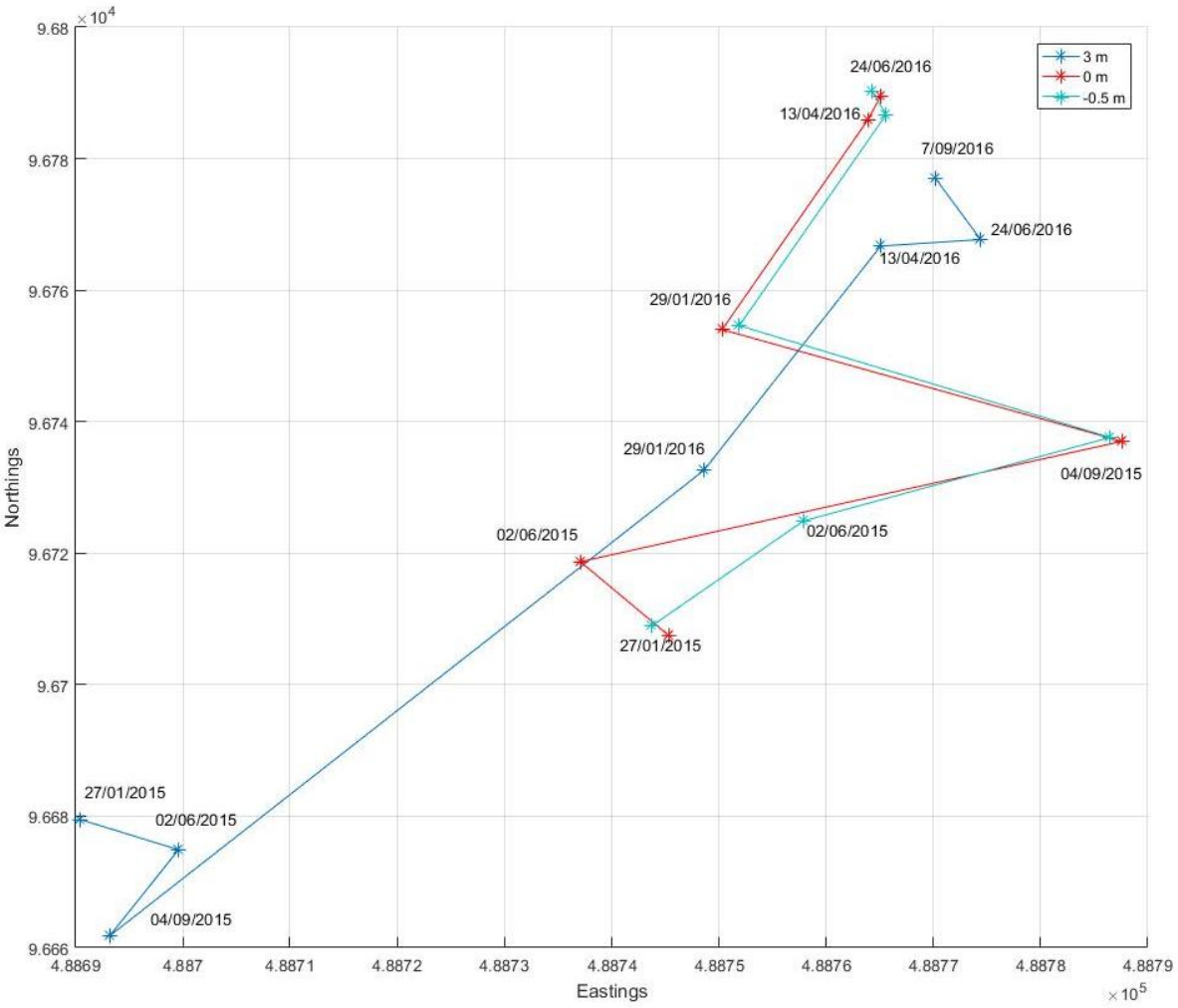

Figure 13- Migration of the distal point of Church Norton spit before the breach and the northern distal point of detached spit post-breach, at elevations of 3 m, 0 m and -0.5 m.

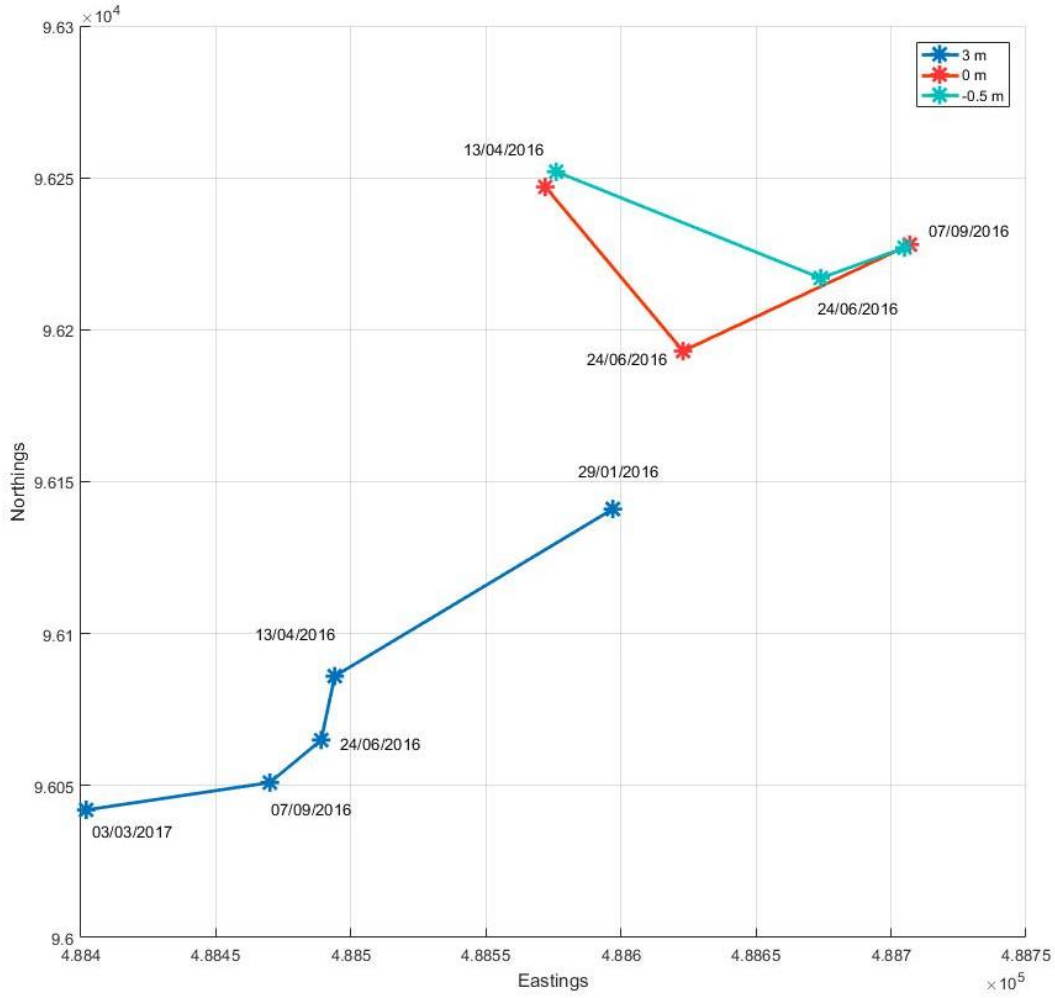

Figure 14- Migration of relic Church Norton spit at elevations of 3 m, 0 m and -0.5 m.

The distal points of 0 and -0.5 m ODN displayed similar behaviour to each other, generally migrating in an offshore direction until 04/09/2015, at which point the distal points migrated back towards the shore and then continued in a north-easterly direction following 29/01/2016. Between 27/01/2015 and 24/06/2016, the 0 m ODN distal point migrated a distance of 83.2 m, while the -0.5 m ODN distal point migrated a distance of 81.1 m between 27/01/2015 and 13/04/2016. Following the 13/04/2016 and 24/06/2016, the -0.5 m and 0 m ODN distal points respectively had fused with the shoreline.

In the period after the breach, the 3 m ODN distal point of the relic church Norton spit was shown to recede along the coastline in a south westerly direction, extending the breach opening in the process. Between 29/01/2016 and 03/03/2017, the 3 m ODN distal point migrated 216.3 m. The 0 m ODN relic spit distal point migrated 128.5 m in the landward direction between 13/04/2016 and 07/09/2016 (Figure 14).

3.1.3. Contour migration

Leading up to the breach, there was a clear section along Church Norton spit where the 3 m contour was noticeably narrower compared to the 3 m contour over the remainder of the spit (Figure 15). This narrowed sectioned section of spit measured 22 m in width, compared to an average width of 42 m over the Church Norton spit. By 29/01/2016, the 3 m contour over this section was discontinuous, indicating that certain sections of the spit crest no longer reached elevations of 3 m. Following the breach, the northern point of the relic spit and the southern tail of the detached spit were shown to deflect shoreward and by 03/03/2017, the 3 m contour fused to the downdrift shoreline.

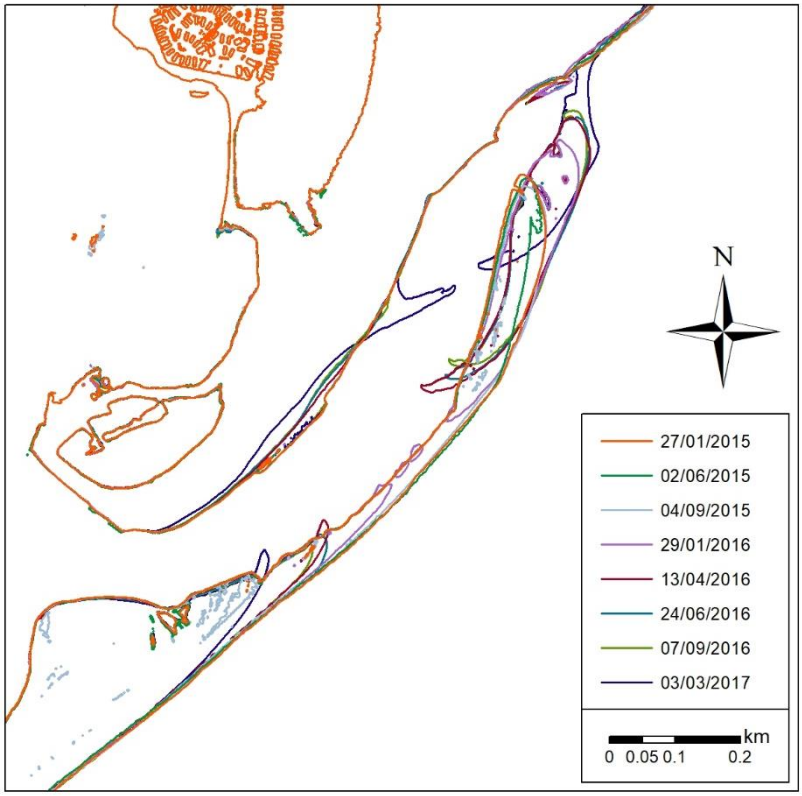

Figure 15: 3 m ODN contour change between 27/01/2015 and 03/03/2017.

3.1.4. Baseline profile volume analysis

The volumes obtained for each baseline profile are described as an area per unit width. Focusing on profiles located along Pagham frontage (Figure 16), immediately downdrift of where the breach occurred, between 27/02/2012 and 29/01/2016, the overall trend displayed for profiles P4d01382 and P4d01377 was a decrease in the area per unit width. Over this period, the volume under these profiles decreased by 25.3 % and 39.1 % respectively. However in the period after the breach from 13/04/2016 to 03/03/2017, profiles P4d01382, P4d01377 and P4d01371 all showed an overall

increase in the area per unit width. Profiles P4d01371 and P4d01377 increased by 14.1 % from 246 m^2/m to 281 m^2/m and 15.4 % from 179 m^2/m to 206 m^2/m respectively, while profile P4d01382 displayed the greatest increase in area per unit width of these three profiles of 34.2 % from 234 m^2/m to 315 m^2/m.

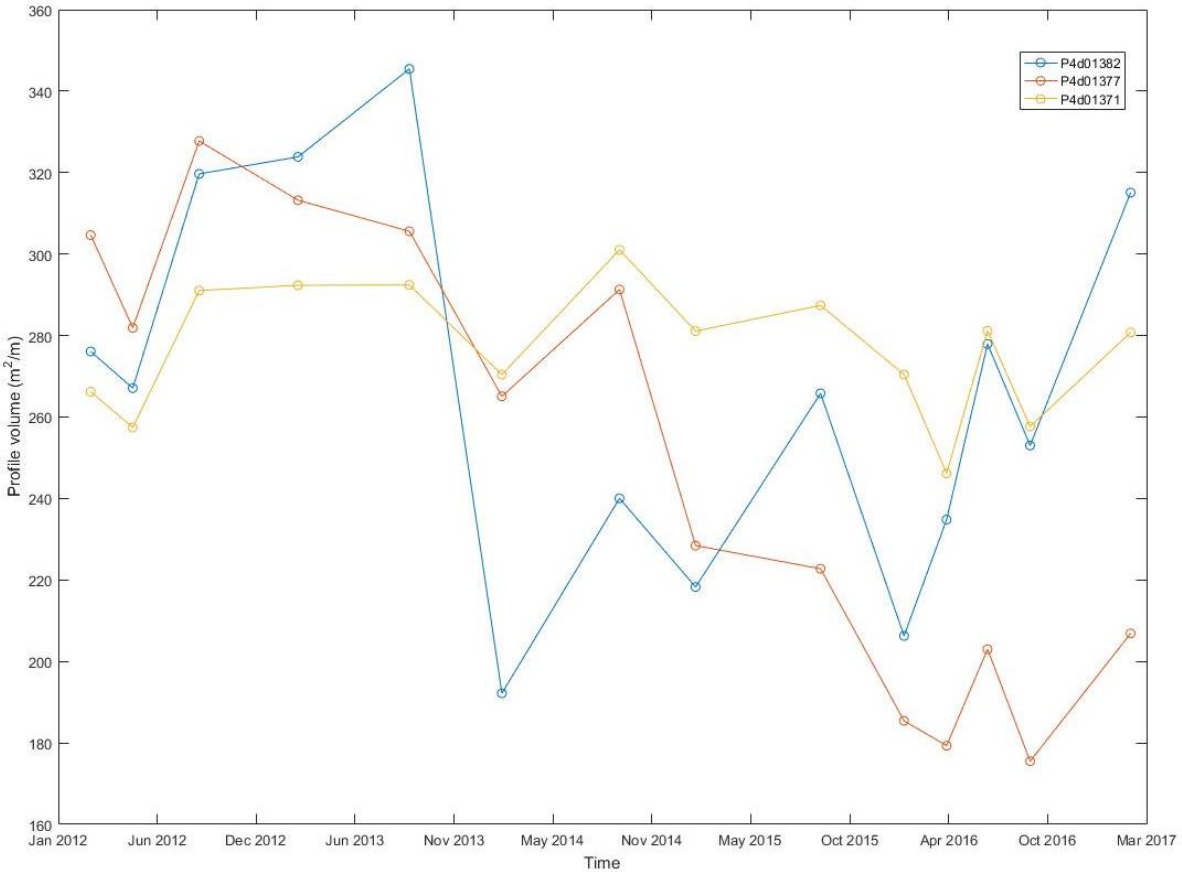

Figure 16- Volume change in baseline profiles P4d01371, P4d01377 and P4d01382 between 05/09/2012 and 03/03/2017.

Comparing the baseline profiles located directly in front of Pagham Harbour, a relatively sharp decrease of 491 m^2/m was shown in profile P4d01391 between 24/06/2016 and 03/03/2017 (Figure 17). In comparison, an increase was observed in profile P4d01387 of 363 m^2/m over the same period.

In terms of the main trends displayed along this section of coastline over the study period, there was a gradual reduction in baseline profiles from P4d01405 to P4d01391 since 2012 (Figure 18). In profiles P4d01397 and P4d01398A, a period of notable reduction in the area per unit width was shown from 2015 onwards (Figure 19). The volume of profile P4d01397 also appeared to fluctuate over the earlier study period from 2012 to 2016, but from June 2016 the volume for this profile started to increase again. However in profiles P4d01359 to P4d01371, located far downdrift of the harbour entrance and P4d01423 to P4d01458, located on the eastern side of Selsey Bill updrift of Pagham, no notable changes in volume were shown since the start of 2012.

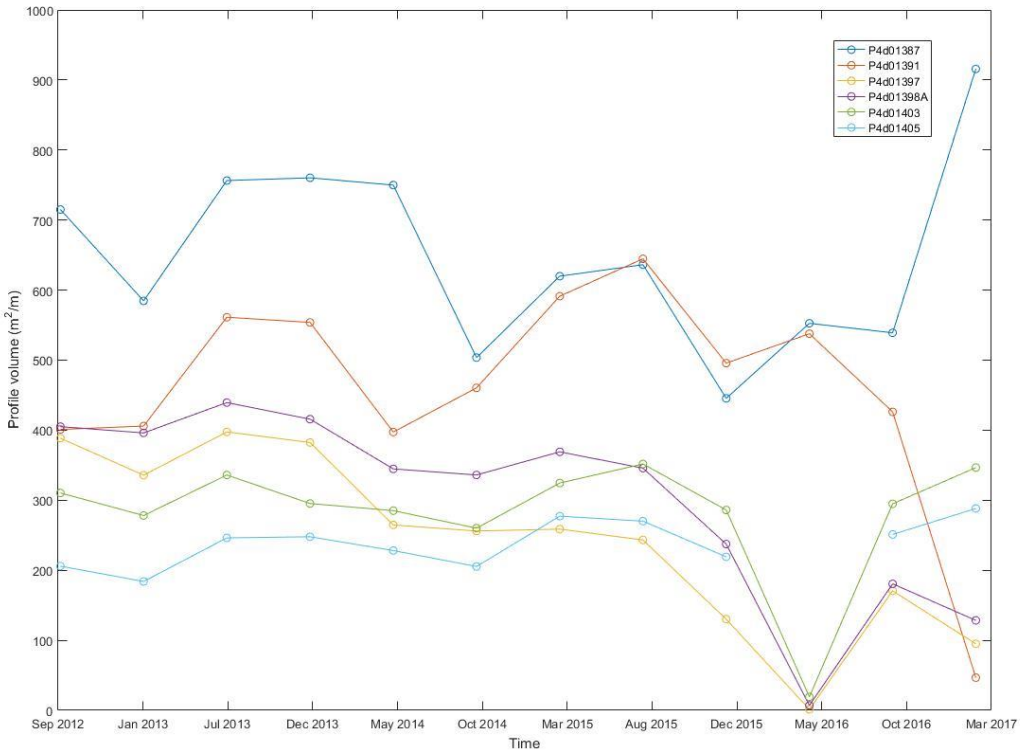

Figure 17- Volume change in baseline profiles P4d01387, P4d01391, P4d01397, P4d01398A, P4d01403 and P4d01405 between 05/09/2012 and 03/03/2017.

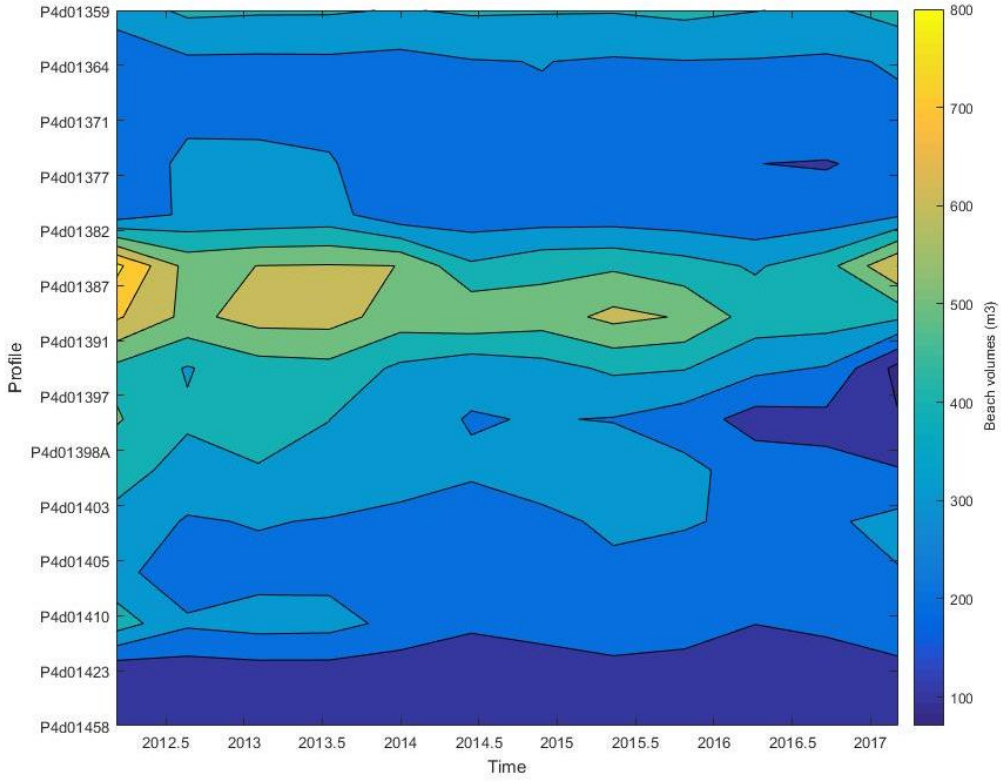

Figure 18- Variation in beach volume across baseline profiles between 2012 and 2017.

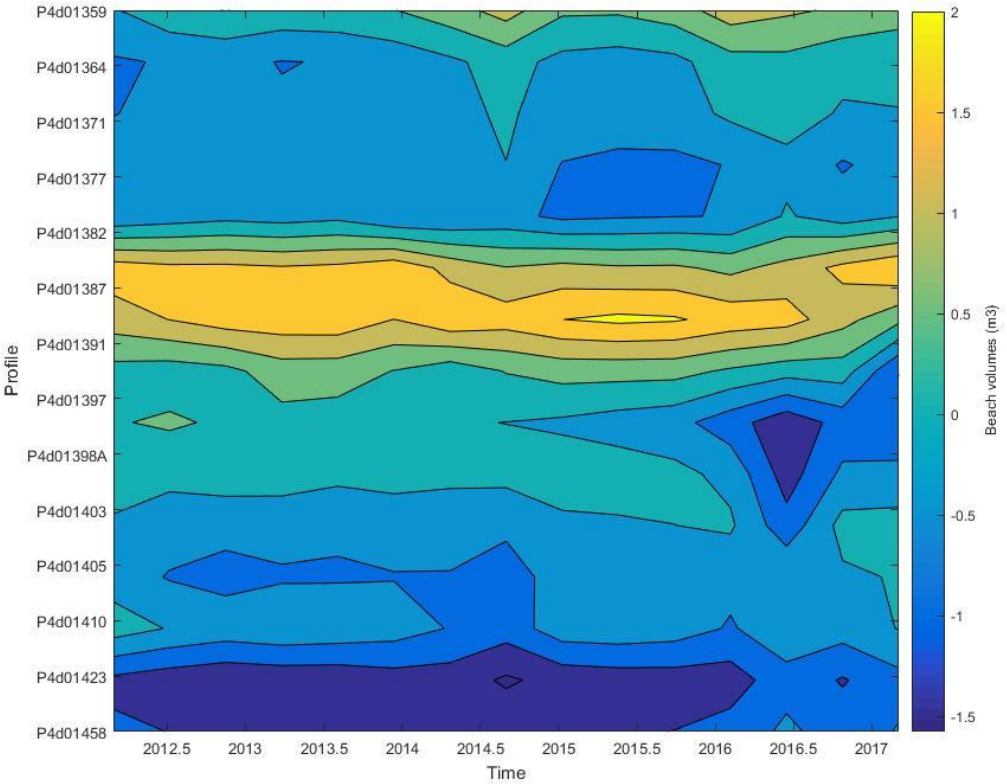

Figure 19- Variation in normalised beach volume across baseline profiles between 2012 and 2017.

3.2. Wave climate analysis

For the following wave climate results, winter was defined as December, January and February.

3.2.1. Significant wave height

Over the time series, from 01/01/2012 to 31/05/2017, the mean significant wave height (H_s) was 0.84 m. From July 2013 to June 2014 and July 2015 to June 2016, similar mean H_s values were obtained of 0.91 m and 0.94 m respectively. However, a larger difference was obtained by comparing the mean H_s values for winter 2013/2014 and winter 2015/2016. For the specific months of December 2013 and January 2014, the mean H_s was 1.46 m, while for December 2015 and January 2016, a higher mean H_s of 1.61 m was observed. However, the maximum H_s recorded in winter 2013/2014 and winter 2015/2016 were similar, with values of 4.01 m and 4.06 m respectively. A monthly mean moving average of H_s is shown in Figure 20.

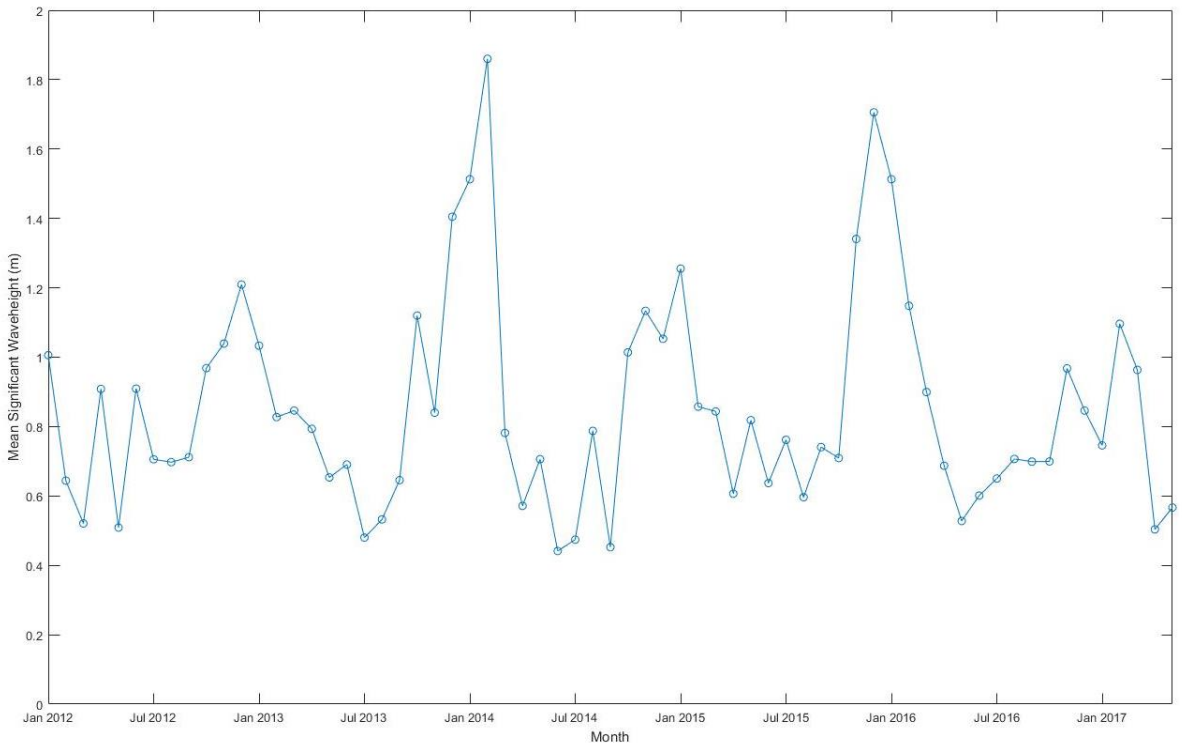

Figure 20- Mean monthly moving average for Hs, between 01/01/2012 and 31/05/2017.

3.2.2. Inshore wave energy flux

Between 01/01/2012 and 31/05/2017, the mean inshore wave energy flux obtained was 1810 J/ms (Figure 21). Comparing the mean inshore wave energy flux over the winter periods, the mean for winter 2014/2015 was 2165 J/ms, while the mean inshore wave energy flux for 2016/17 was 1789

J/ms, which was lower than the mean obtained for the entire timeseries. In comparison, significantly higher values were obtained for winters 2013/2014 and 2015/2016 of 5847 J/ms and 4310 J/ms respectively, with the mean in winter 2013/2014 35.7% higher than in winter 2015/2016. Comparing the maximum inshore energy flux for winters 2013/2014, 2014/2015 and 2015/2016, the highest energy fluxes shown were 6.60×10^4 J/ms in December 2013, 3.40×10^4 J/ms in January 2015 and 3.97×10^4 J/ms in December 2015.

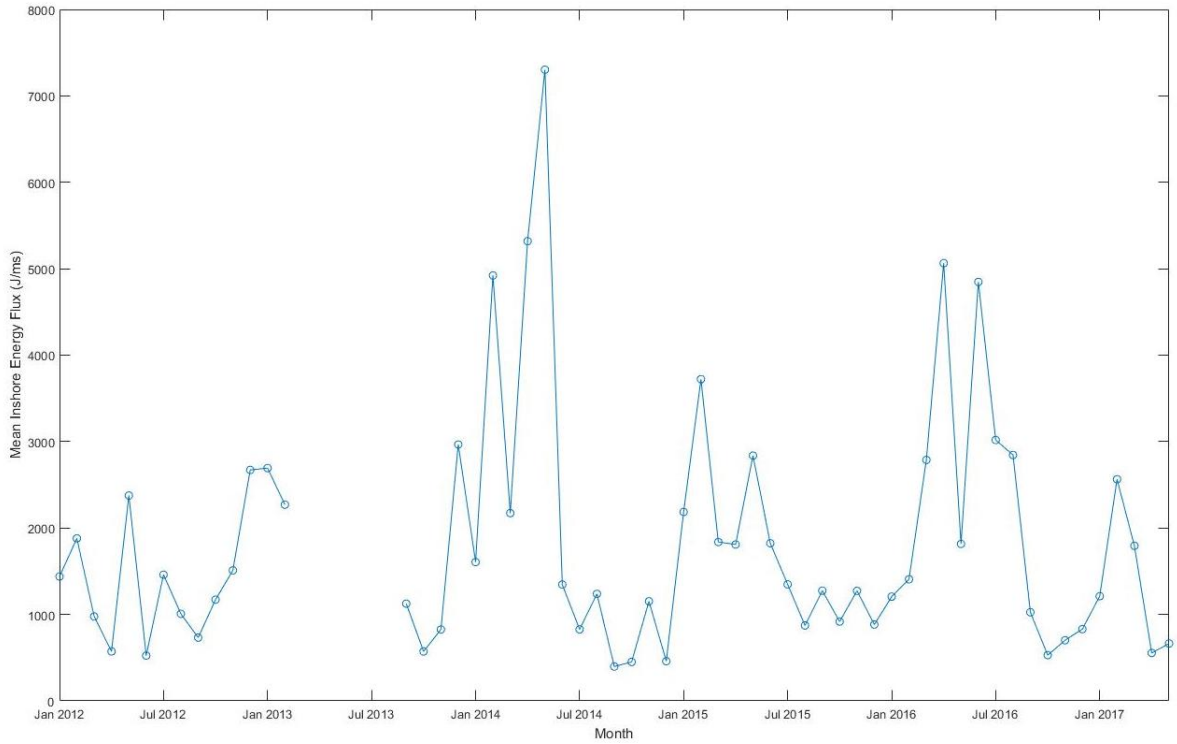

Figure 21- Mean monthly moving average for inshore wave energy flux between 01/01/2012 and 31/05/2017.

3.2.3. Ratio of longshore to cross-shore energy flux

The monthly mean longshore to cross-shore transport (LsXs) ratio is shown in Figure 22. There are clear fluctuations in the monthly mean transport ratio, particularly the downward fluctuations in the ratio getting progressively larger between 2013 and 2015, while the peak monthly mean transport ratios obtained remain relatively similar. The mean ratios were obtained for winter 2013/2014 and winter 2015/2016 were similar with values of 0.63 and 0.64 respectively. The lowest mean transport ratio occurred in October 2015 with a value of 0.40, before increasing to 0.67 in November 2015 and 0.69 in December 2015. In comparison, the ratios obtained for October and November 2015 were 0.57 and 0.55 respectively. The ratio was 41.4 % higher in October 2013 than October 2015, however the ratio was 21.3 % higher in November 2015 than November 2013.

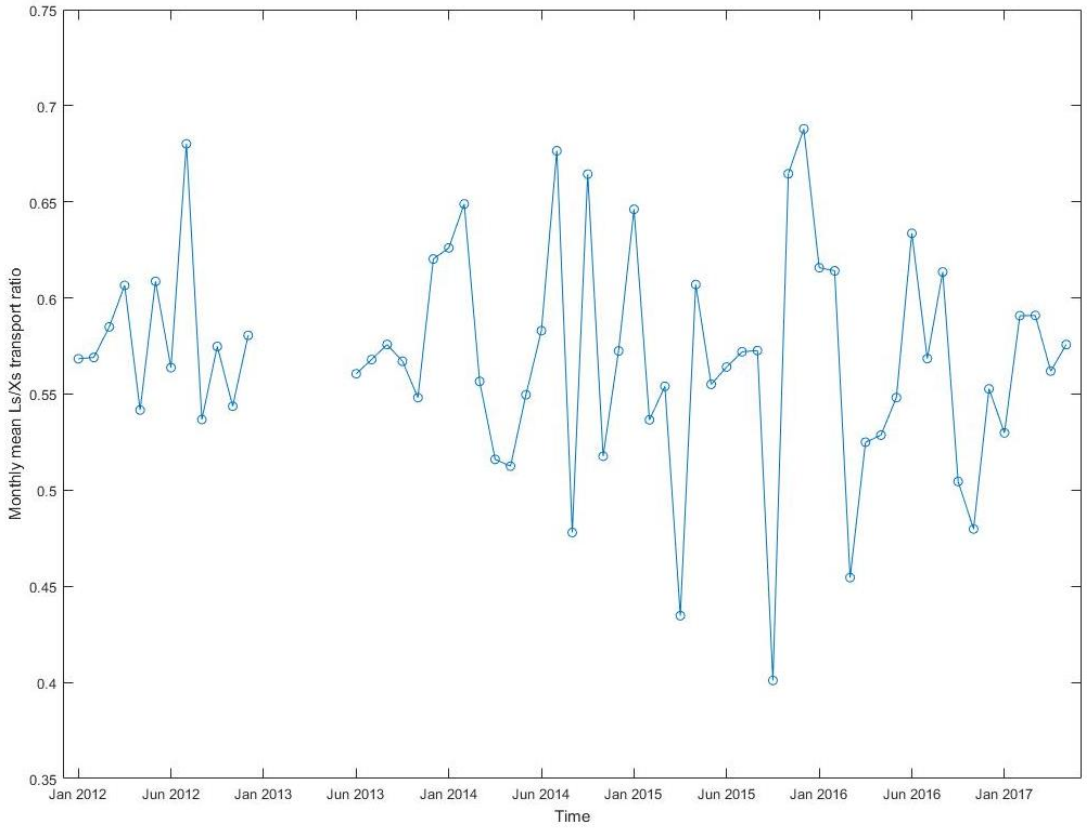

Figure 22- Mean monthly moving average for the longshore to cross-shore transport ratio, between 01/01/2012 and 31/05/2017.

3.2.4. Peak wave period

The mean peak wave periods (T_p) measured at the Rustington wave buoy was 6.85 s, between 01/01/2012 and 31/05/2017 (Figure 23). From July 2013 to June 2014 and July 2015 to June 2016, similar mean T_p values were obtained of 6.85 s and 6.79 s respectively. Comparing winter 2013/2014 and winter 2015/2016, the mean T_p was similar, with values obtained of 8.40 s for winter 2013/2014 and 8.41 s for winter 2015/2016. However, the maximum T_p recorded was higher in winter 2013/2014 than winter 2015/2016, with a maximum peak wave period in December of 28.6 s and January of 18.2 s respectively.

3.2.5. Wave direction

For the period from July to June, for 2013/2014, 2014/2015 and 2015/2016, no significant variations in the mean wave direction were obtained. For these periods, the mean wave direction was 197.1˚, 196.5 ˚ and 195.7 ˚ respectively. During winter 2013/2014, 2014/2015 and 2015/2016, the mean wave directions obtained were similar (Figure 24). The mean wave direction for 2013/2014 was 203.4 ˚, 202.3 ˚ in 2014/2015 and 204.9 ˚ in 2015/2016.

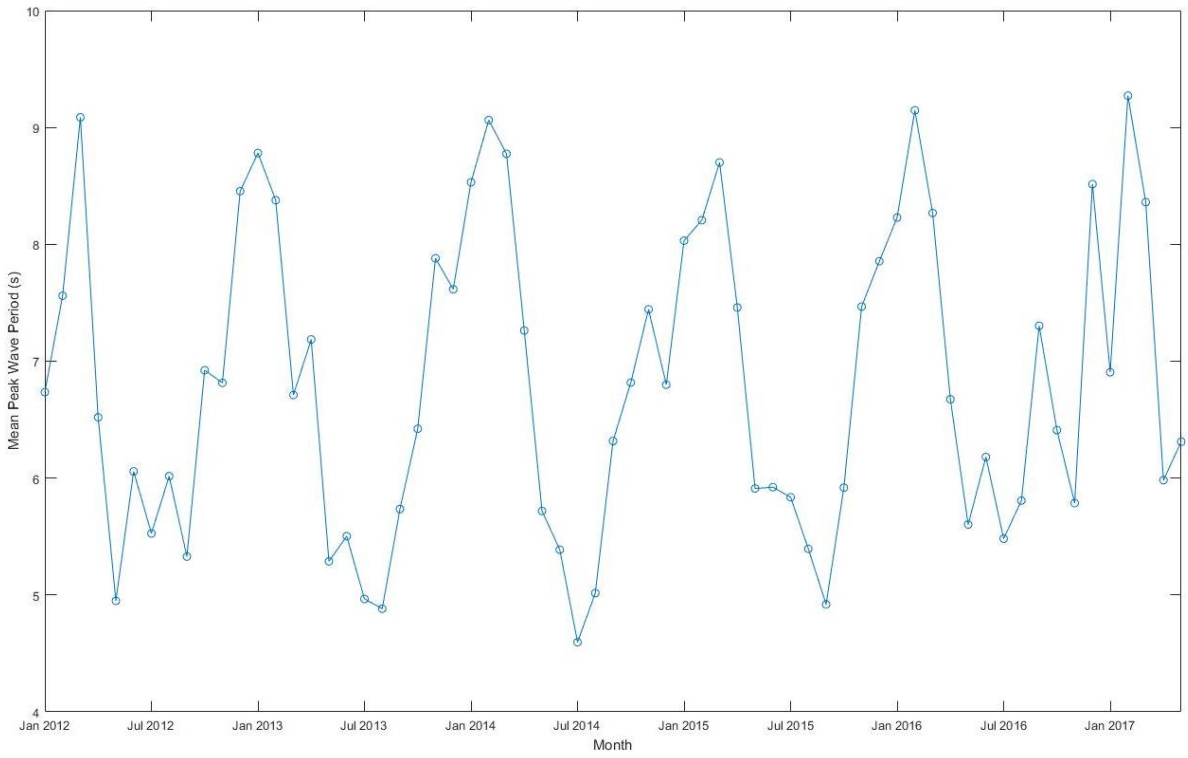

Figure 23- Mean monthly moving average for Tp between 01/01/2012 and 31/05/2017.

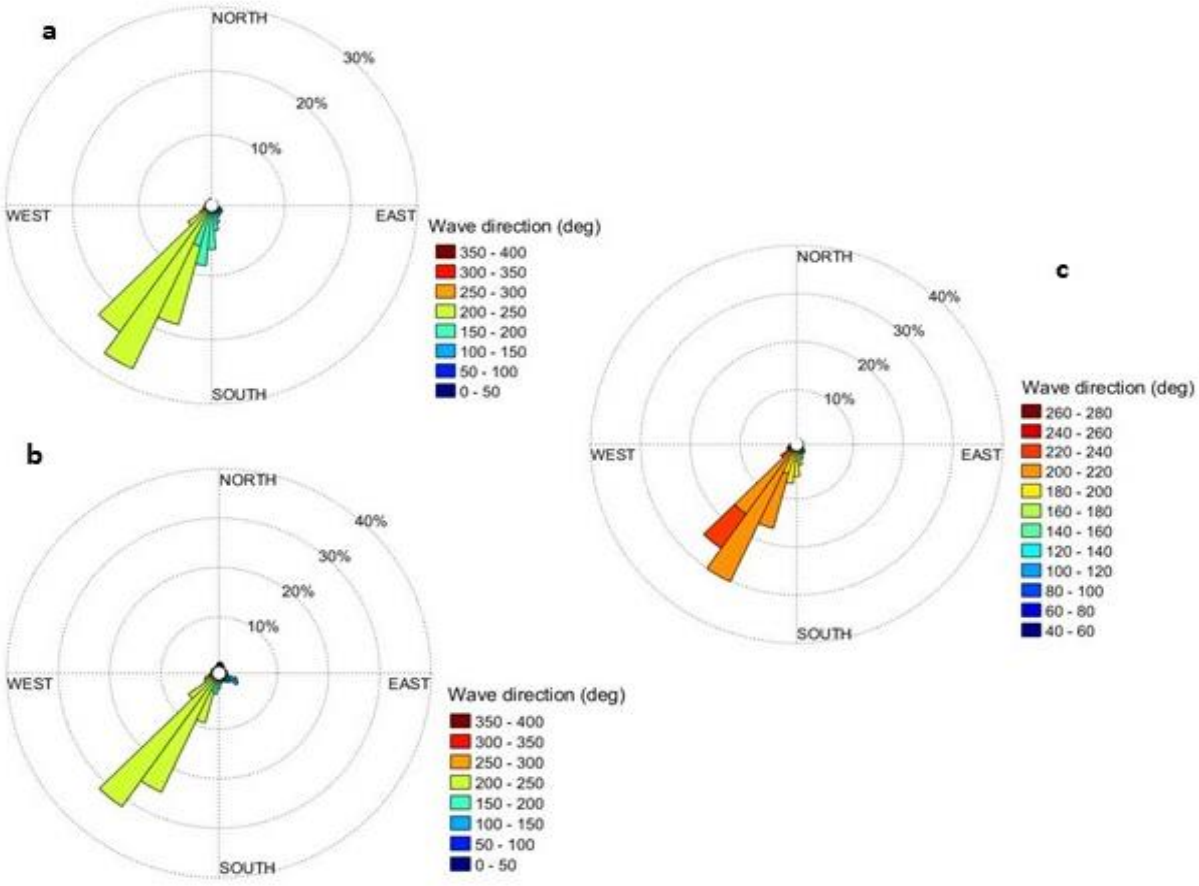

Figure 24- Mean wave direction for (a) winter 2013/2014, (b) winter 2014/2015 and (c) winter 2015/2016.

3.3. Overtopping volume

Comparing the winters of 2013/2014, 2014/2015 and 2015/2016 the highest mean overtopping volume obtained was 1.21×10^{-5} m^3 in 2013/2014, which was two orders of magnitude greater than the mean overtopping volume from 2015/2016 and four orders of magnitude greater than the same period in 2014/2015. For these winters, the mean overtopping volumes determined were $7.51 \times 10^{-9} m^3$ and $3.94 \times 10^{-7} m^3$ for 2014/2015 and 2015/2016 respectively. In terms of the maximum overtopping volumes obtained for each of these periods, the maximum overtopping volumes occurred in November 2013 and 2014, with volumes of 0.153 m^3 and 8.51×10^{-5} m^3 respectively and January 2016, with a volume of 1.23×10^{-4} m^3.

3.4. Littoral drift potential

Since 01/01/2012 there have been two notable peaks in the total monthly littoral drift volumes, corresponding with winter 2013/2014 and winter 2015/2016 (Figure 25). The largest peak occurred in February 2014, with an estimated total drift volume in February of 1.33×10^4 m^3, while the second significant peak occurred in December 2015, where a total drift volume of 1.05×10^4 m^3 was shown. Between July 2013 and June 2014, a total drift volume of 4.35×10^4 m^3 was obtained, however for the same period in 2015/2016, a lower total drift volume of 3.37×10^4 m^3 was shown. Between July 2014 to June 2015, the total drift volume was smaller again, with an estimated volume of 2.11×10^4 m^3.

Year	Total Annual Drift Volume (m^3/yr)
2008[x]	1.88×10^4
2009[x]	2.35×10^4
2010[x]	1.21×10^4
2011[x]	1.51×10^4
2012	1.44×10^4
2013[x]	2.80×10^4
2014	3.79×10^4
2015	2.71×10^4
2016	2.23×10^4
2017*	5.34×10^3

Table 5- Total annual drift volumes between 2008 and 2017 (January to May only; x value obtained from Townend (2015).*

Comparing the estimated total annual drift volume over the study period, the greatest total drift potential was displayed in 2014 measuring 3.79x10^4 m^3/yr (Figure 26). Since 2010 the drift potential generally increased up until 2014, after which the drift potential decreased rapidly. Table 5 contains a summary of the total annual drift volumes between 2008 and 2017.

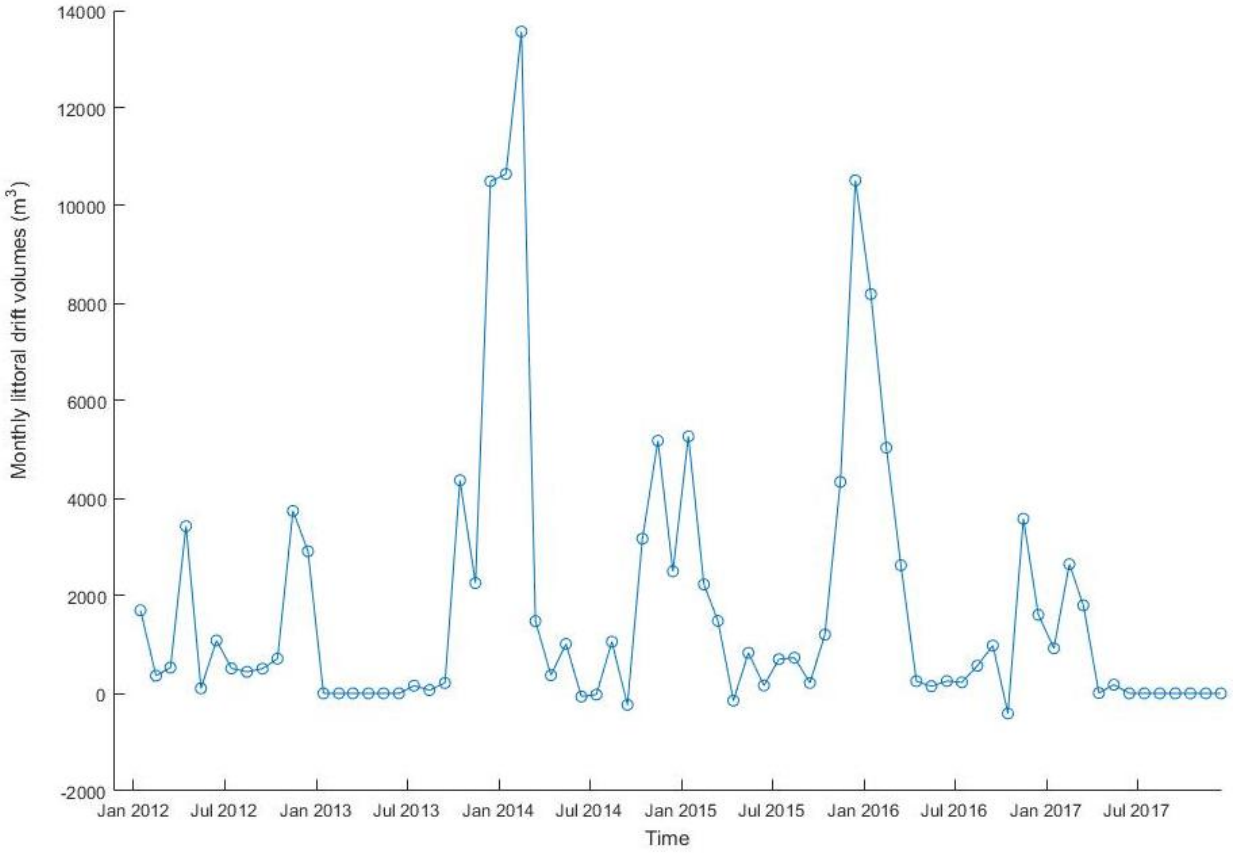

Figure 25- Monthly littoral drift volume between January 2012 to May 2017.

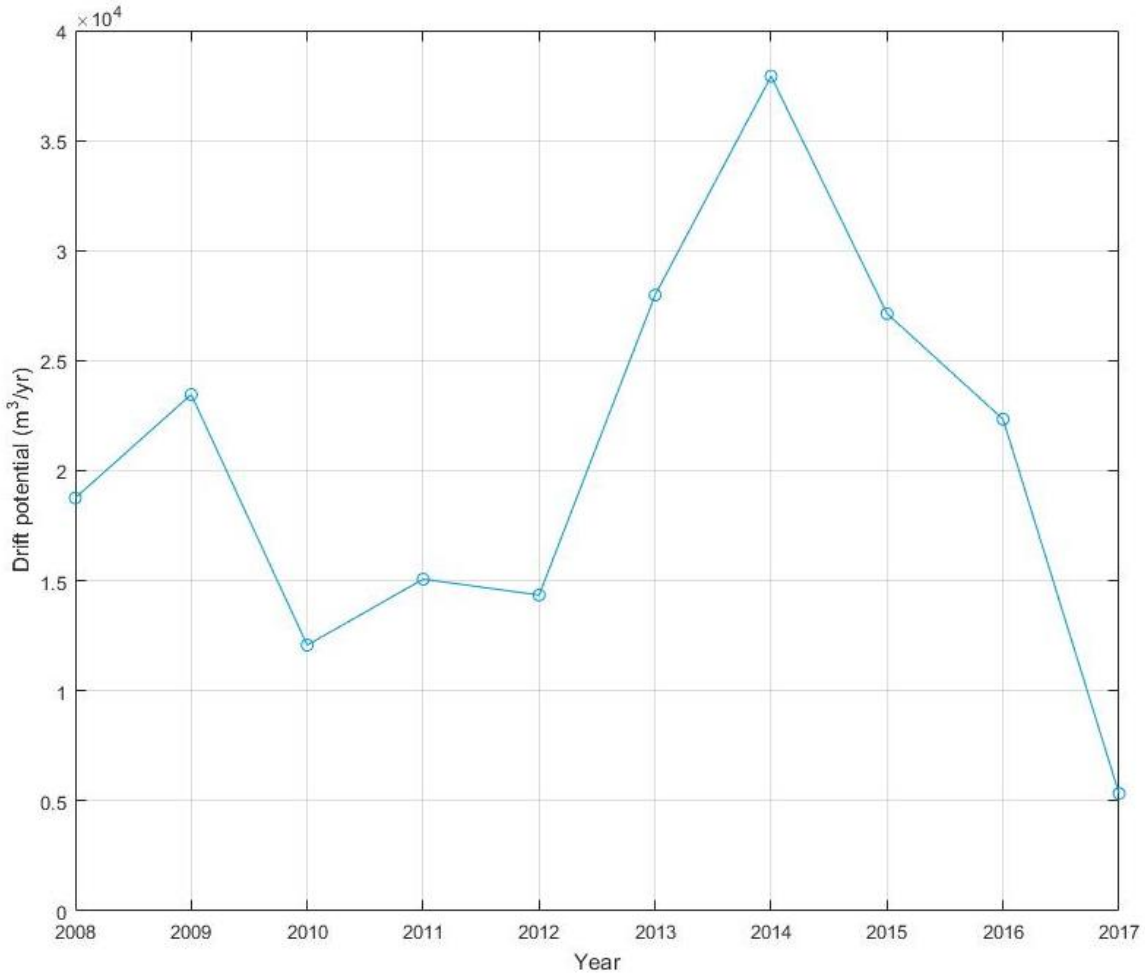

Figure 26- Annual littoral drift volume potential from 2008 to May 2017. Note: The drift volume obtained for 2017 only accounts for January to May. Values for 2008-2011 and 2013 sourced from Townend (2015).

3.5. Overtopping and overwash model

The model results for the crest elevation display similar behaviour to that shown in the GIS analysis, with the crest level reducing gradually over the year prior to the breach. During winter 2013/2014, the model indicated two small episodic periods where the crest level lowered marginally from 5 m ODN to 4.75 m ODN and 4.64 m ODN on 06/11/2013 and 06/01/2014 respectively (Figure 27). However, these periods were relatively short-lived and the crest level generally recovered back to the maximum crest level defined in the model shortly afterwards. The corresponding H_s that occurred during these two episodic lowering events on 06/11/2013 and 06/01/2014 were 6.32 m and 3.01 m respectively, while the corresponding T_p for both events was greater than 22 seconds. In terms of the estimated inshore wave energy flux, the estimated value was significantly greater on the 06/11/2013 compared to the 06/01/2014, with values obtained of 1.11×10^5 J/ms on 06/11/2013 and 3.65×10^4 J/ms on 06/01/2014 (Table 6).

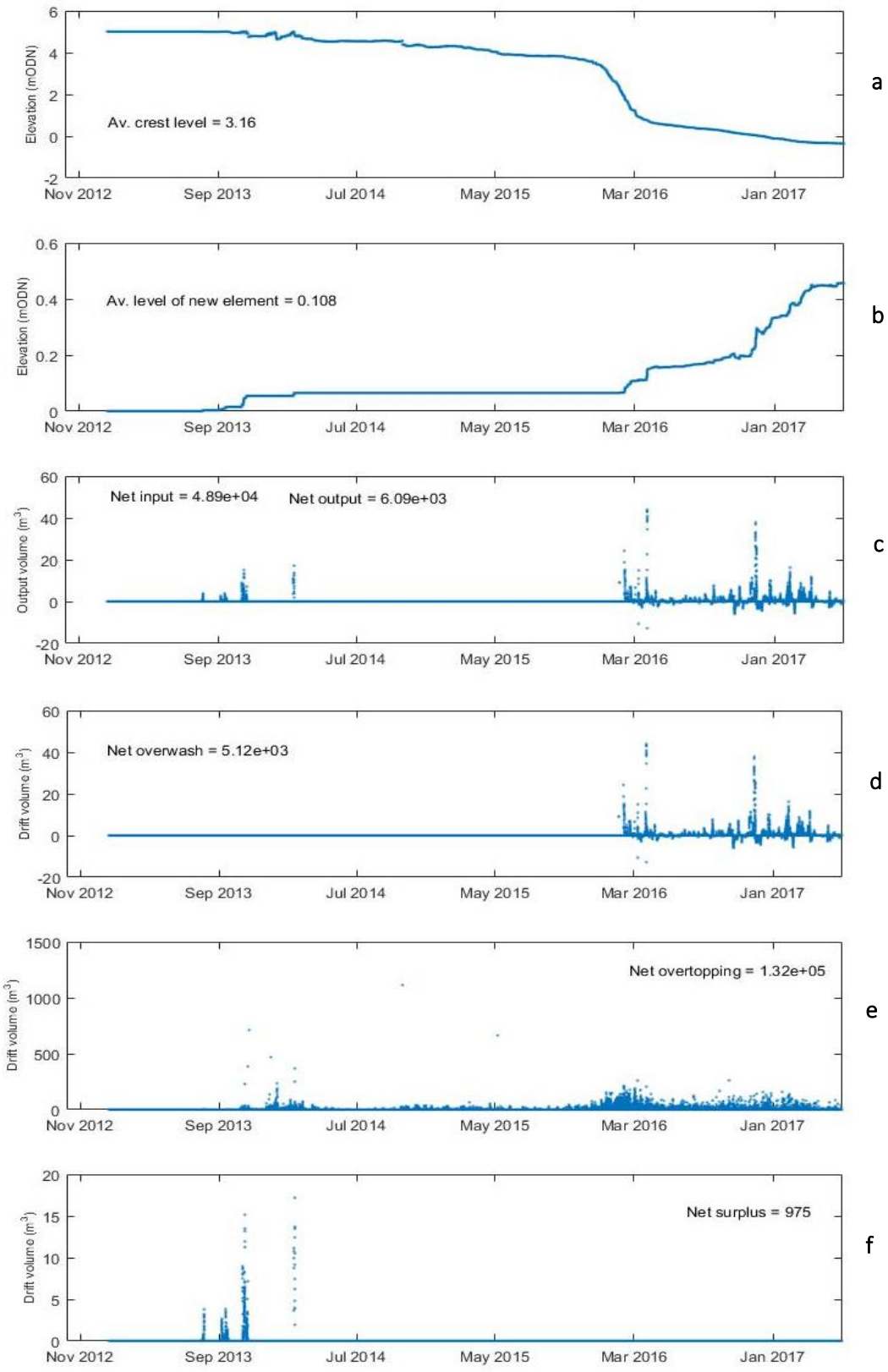

Figure 27- Overtopping-overwash model of Church Norton spit: (a) Crest level; (b) Level of new element; (c) Net input and output; (d) Overwash volume; (e) Overtopping volume; (f) Surplus sediment volume.

A third period of lowering was also observed to start midway through February 2014, on 14/02/2014, however the crest did not recover and the model indicated a continual downward trend in the crest level following this lowering. On 14/02/2014 the H_s obtained was 10.7 m, the T_p was greater than 20 seconds and the estimated inshore wave energy flux was $6.57x10^4$ J/ms. From December 2015 to February 2016, a rapid decrease in the crest level was shown from approximately 3.5 m ODN to 1 m ODN. In this period, the T_p values obtained were notably high, with values frequently greater than 18 seconds and values of H_s were on the order of 3.5 to 4.1 m. Furthermore, for the three dates in which crest lowering events were noted, the corresponding high tide levels was 3.04 m ODN on the 06/11/2013, 2.42 m ODN on the 06/01/2014 and 3.36 m ODN on 14/02/2014.

Date of crest lowering event	H_s (m)	T_p (s)	Inshore wave energy flux (J/ms)	High water level (m ODN)
06/11/2013	6.32	22.2	$1.11x10^5$	3.04
06/01/2014	3.01	25.0	$3.65\ x10^4$	2.42
14/02/2014	10.7	25.0	$6.57x10^4$	3.36

Table 6- A summary of Hs (m), Tp (s), inshore wave energy flux (J/ms) and highwater level (m) corresponding to crest lowering events indicated by the spit overtopping and overwash model.

Date of overwash event	H_s (m)	T_p (s)	Inshore wave energy flux (J/ms)
27/01/2016	3.25	11.8	$2.20x10^4$
06/02/2016	3.95	10.5	$3.46\ x10^4$
07/02/2016	4.06	10.5	$1.05\ x10^4$
08/02/2016	3.98	18.2	$2.74\ x10^4$
19/02/2016	2.30	18.2	$1.20\ x10^4$
09/03/2016	3.78	9.1	$7.17\ x10^4$
28/03/2016	7.99	28.6	$1.01\ x10^5$

Table 7- A summary of Hs (m), Tp (s) and inshore wave energy flux (J/ms) corresponding to the highest volume overwash events in winter 2013/2014 and 2015/2016.

Date of overtopping event	H_s (m)	T_p (s)	Inshore wave energy flux (J/ms)
28/10/2013	6.93	25.0	$5.68x10^4$
03/11/2013	5.34	25.0	$6.40 x10^4$
06/11/2013	6.32	22.2	$1.11x10^5$
24/12/2013	14.3	28.6	$6.60x10^4$
06/01/2014	3.01	25.0	$2.81x10^4$
14/02/2014	10.7	25.0	$6.57x10^4$
31/12/2015	3.79	18.2	$3.97x10^4$
14/01/2016	1.74	9.10	$2.58x10^4$
06/02/2016	3.95	10.5	$3.46x10^4$
08/02/2016	3.98	18.2	$2.74x10^4$

Table 8- A summary of Hs (m), Tp (s) and inshore wave energy flux (J/ms) corresponding to the highest volume overtopping events in winter 2013/2014 and 2015/2016.

In terms of overwash, which can be defined as the flow of water and sediment over the top of the beach crest with no direct return route back to the initial water body (Donnelly *et al.,* 2006), the model results showed that no overwash occurred prior to January 2016. The first occurrence of overwash occurred on 27/01/2016, coinciding with the start of the rapid decrease observed in the crest level and had an estimated overwash volume of 8.97 m^3. On this date, the estimated crest height was 2.30 m while the high tide water level was 2.83 m. Between 01/01/2016 and 31/05/2017, the estimated net overwash was $5.12x10^3$ m^3, of which 18.2 m^3 occurred in January 2016 and a significantly larger volume of 488 m^3 occurred in February 2016. Table 7 summarises the H_s, T_p and inshore wave energy flux corresponding to the highest volume overwash events in winter 2015/2016.

Overtopping was shown to occur frequently over the period the model was run. The single maximum overtopping for winter 2013/2014 was 712 m^3 and occurred on 06/11/13, while the maximum overtopping for winter 2015/2016 was 210 m^3 and took place on 08/02/2016. The key difference shown in overtopping volumes between winter 2013/2014 and winter 2015/2016 was that although winter 2013/2014 indicated events with greater overtopping volumes, the overtopping in winter 2015/2016 was more intense and frequent (Figure 26).

However the model output also indicates overtopping events occurring throughout 2014 and 2015, including the summer months, yet no overtopping events were indicated before winter 2013/2014.

Table 8 summarises the H_s, T_p and inshore wave energy flux corresponding to the highest volume overtopping events in winter 2013/2014 and 2015/2016.

3.5.1. Model sensitivity analysis

Model properties	Model run						
	A	B	C	D	E	F	G
Element width (m)	150	150	150	150	150	150	150
Element length (m)	200	200	200	200	200	200	200
Bed level (m ODN)	-0.5	-0.5	-0.5	-0.5	-0.5	-0.5	-0.5
Initial crest level (m ODN)	5	5	5	5	5	5	5
Max crest level (m ODN)	5	5	5	5	5	5	5
Crest width (m)	20	20	20	10	40	20	20
Spit slope (1:m)	6	6	6	6	6	4	8
Roughness	1	1	1	1	1	1	1
Overtopping transport coefficient (K_0)	10	50	200	17	17	17	17

Table 9- Model parameters used in the overtopping-overwash model sensitivity analysis.

Throughout this sensitivity analysis, the element width, length and bed level were kept constant as these dimensions were considered similar to the cell dimensions used in the GIS volume analysis. A summary of model parameters used in the sensitivity analysis are shown in Table 9 and model sensitivity analysis results are shown in Table 10.

	Model run						
	A	B	C	D	E	F	G
Av. crest level (m ODN)	4.90	0.72	0.52	1.69	4.71	4.17	3.23
Av. Level of new element (m ODN)	0.761	1.29	1.76	0.45	0.12	0.12	0.15
Net input volume (m^3)	$4.89x10^4$	$4.89x10^4$	$4.89x10^4$	$4.89x10^4$	$4.89x10^4$	$4.89x10^4$	$4.89x10^4$
Net output volume (m^3)	$2.04x10^4$	$3.34x10^4$	$3.89x10^4$	$1.92x10^4$	$3.25x10^4$	$2.62x10^3$	$6.25x10^3$
Net overwash (m^3)	0	$3.34x10^4$	$3.89x10^4$	$1.84x10^4$	0	400	$4.48x10^3$
Net overtopping (m^3)	$2.99x10^4$	$1.08x10^5$	$1.03x10^5$	$1.16x10^5$	$5.82x10^4$	$1.06x10^5$	$1.31x10^5$
Net surplus (m^3)	$2.04x10^4$	38.4	0.19	791	$3.25x10^3$	$2.22x10^3$	$1.77x10^3$

Table 10- Overtopping-overwash model sensitivity analysis results.

In model run A (Figure 28), when the overtopping transport coefficient was lowered to 10, the average crest level of the element was 55 % higher, the net volume of overtopping was $1.02x10^5$ m^3 lower and no overwash occurred. In comparison, when the overtopping transport coefficient was increased to 50, in model run B (Figure 29) and 200, in model run C (Figure 30), the average crest level reduced by 77.2 % and 83.5 % respectively and the net overtopping volumes were on the same order of magnitude. Additionally, the average level of the new element increased by 1094 % in model run B and 1529 % in model run C.

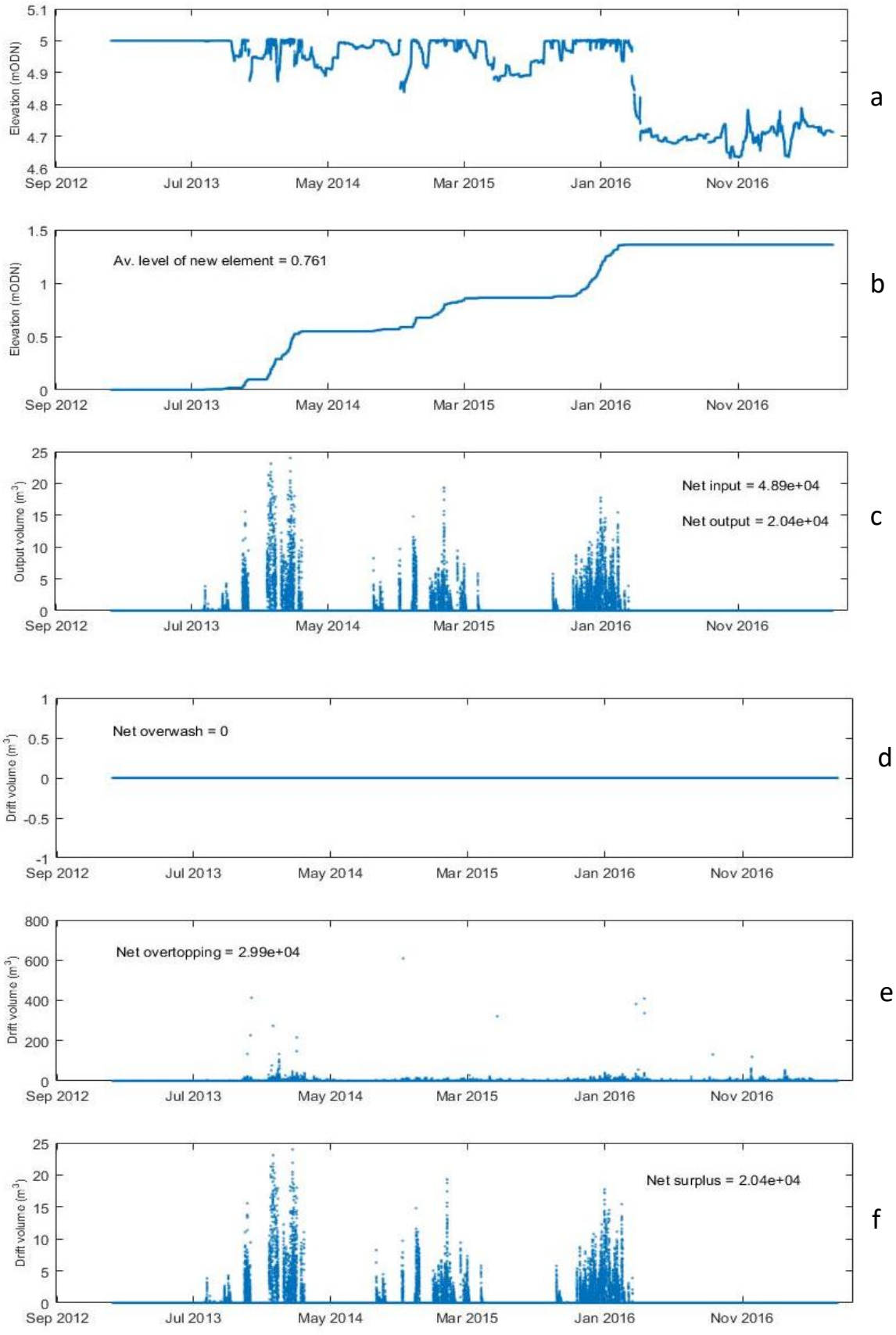

Figure 28- Sensitivity model run A: (a) Crest level; (b) Level of new element; (c) Net input and output; (d) Overwash volume; (e) Overtopping volume; (f) Surplus sediment volume.

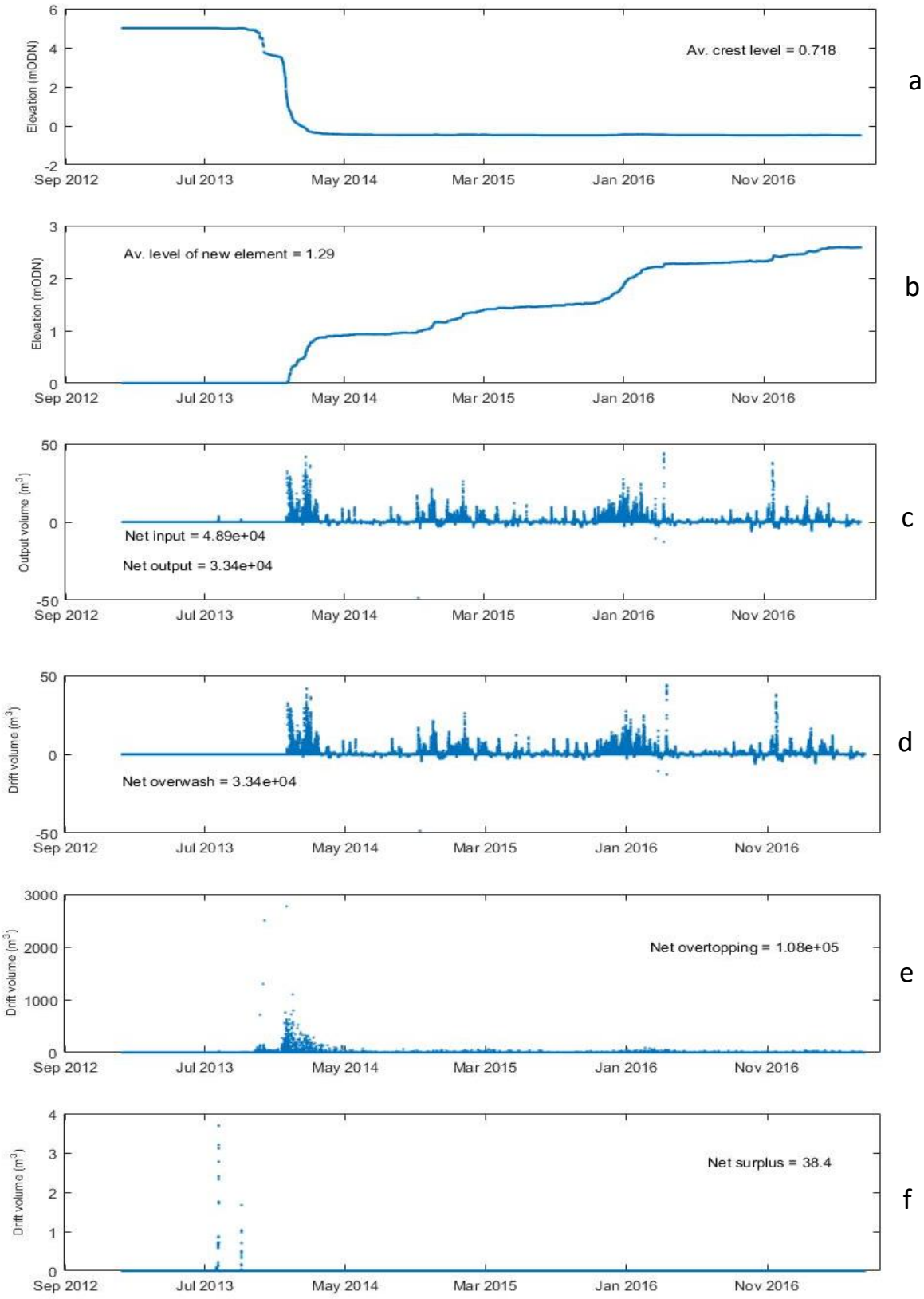

Figure 29- Sensitivity model run B: (a) Crest level; (b) Level of new element; (c) Net input and output; (d) Overwash volume; (e) Overtopping volume; (f) Surplus sediment volume.

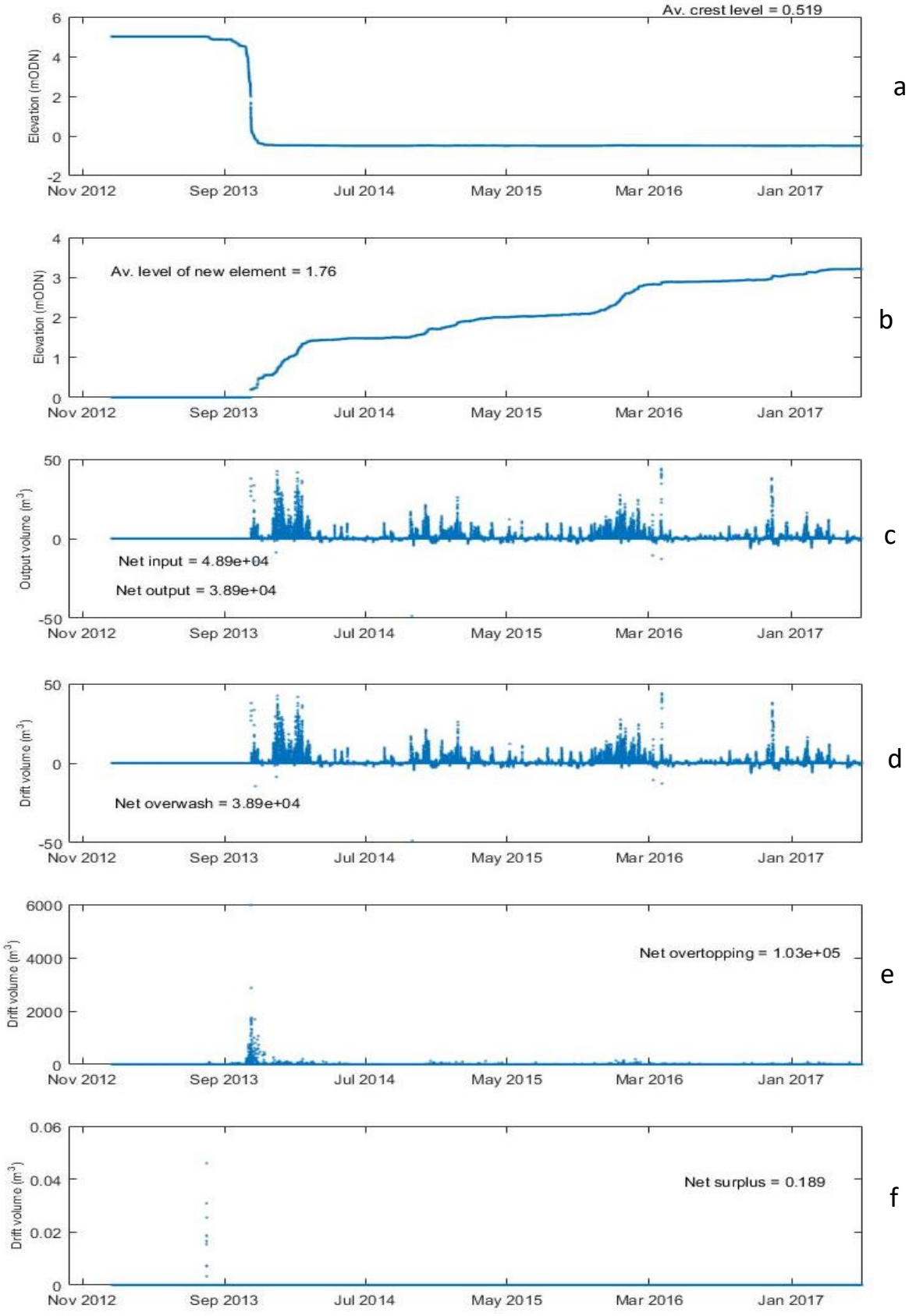

Figure 30- Sensitivity model run C: (a) Crest level; (b) Level of new element; (c) Net input and output; (d) Overwash volume; (e) Overtopping volume; (f) Surplus sediment volume.

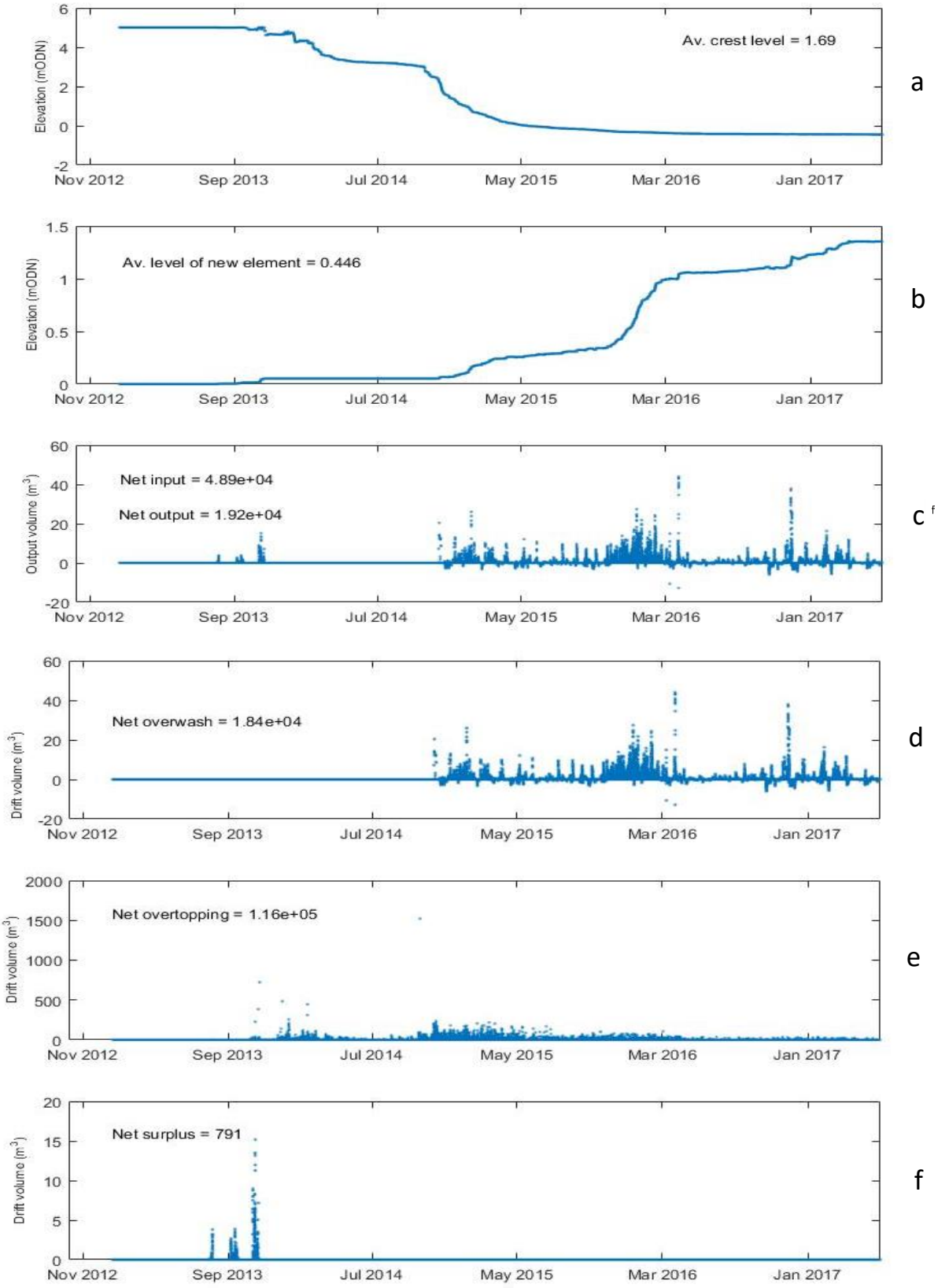

Figure 31- Sensitivity model run D: (a) Crest level; (b) Level of new element; (c) Net input and output; (d) Overwash volume; (e) Overtopping volume; (f) Surplus sediment volume.

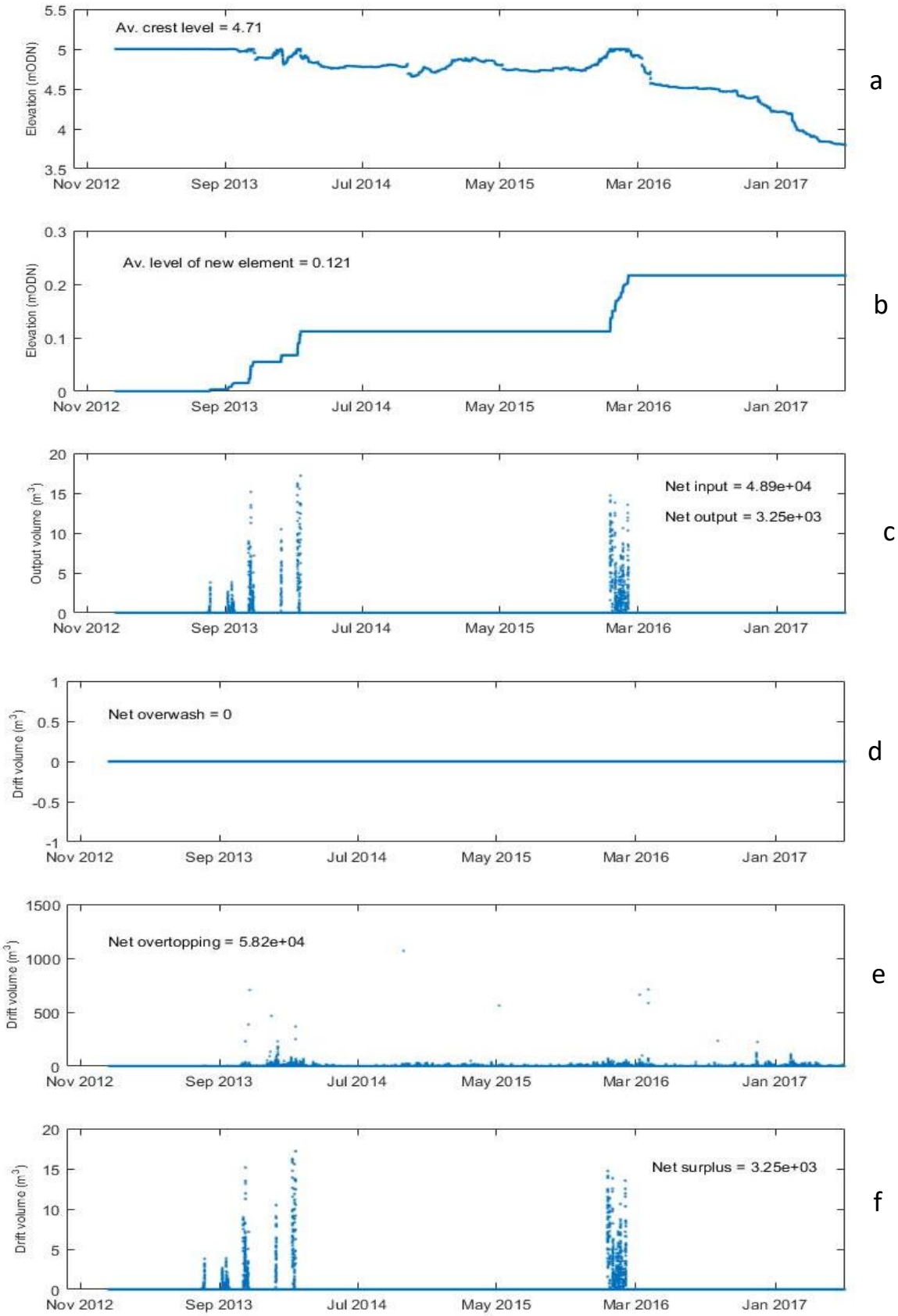

Figure 32- Sensitivity model run E: (a) Crest level; (b) Level of new element; (c) Net input and output; (d) Overwash volume; (e) Overtopping volume; (f) Surplus sediment volume.

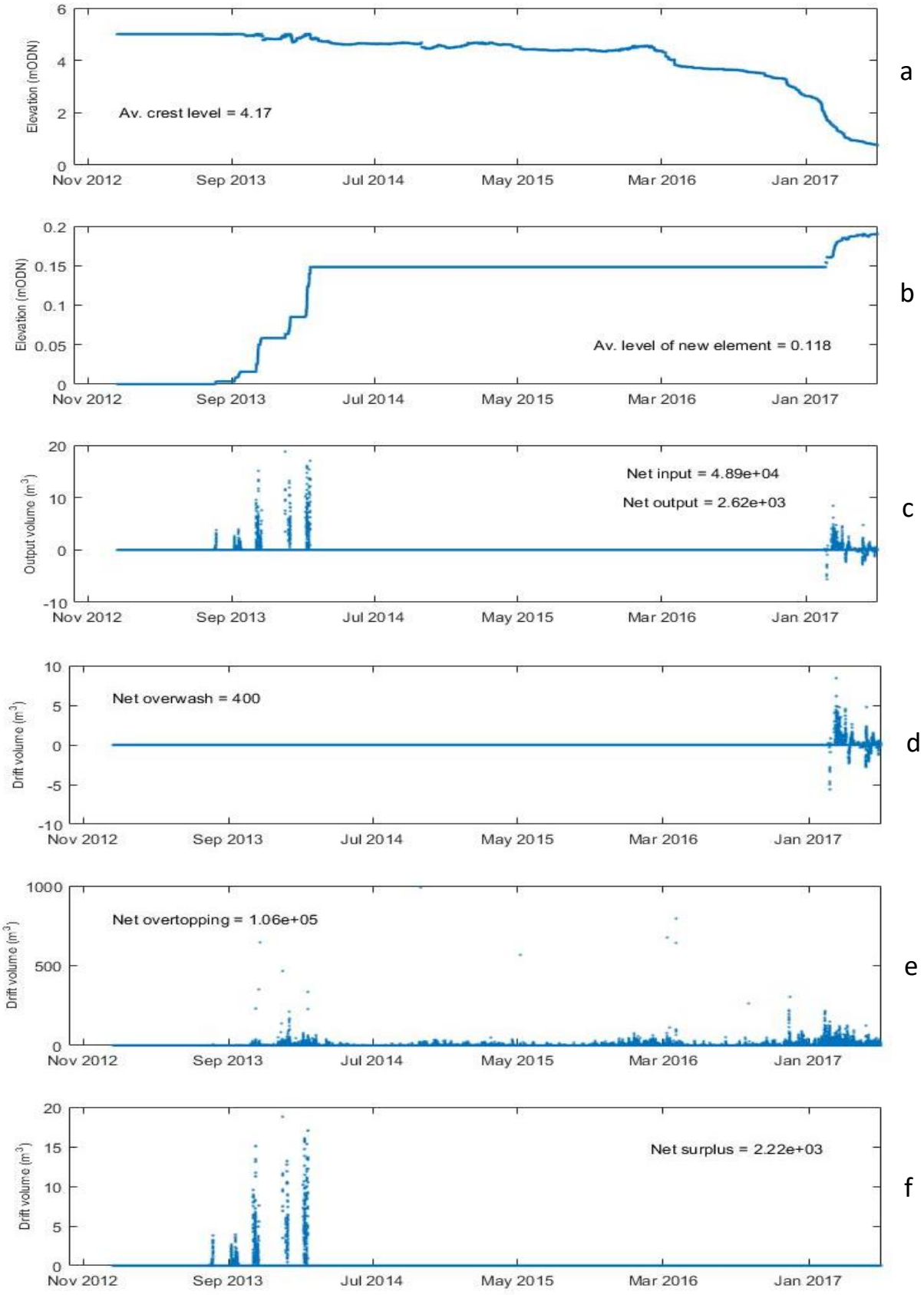

Figure 33- Sensitivity model run F: (a) Crest level; (b) Level of new element; (c) Net input and output; (d) Overwash volume; (e) Overtopping volume; (f) Surplus sediment volume.

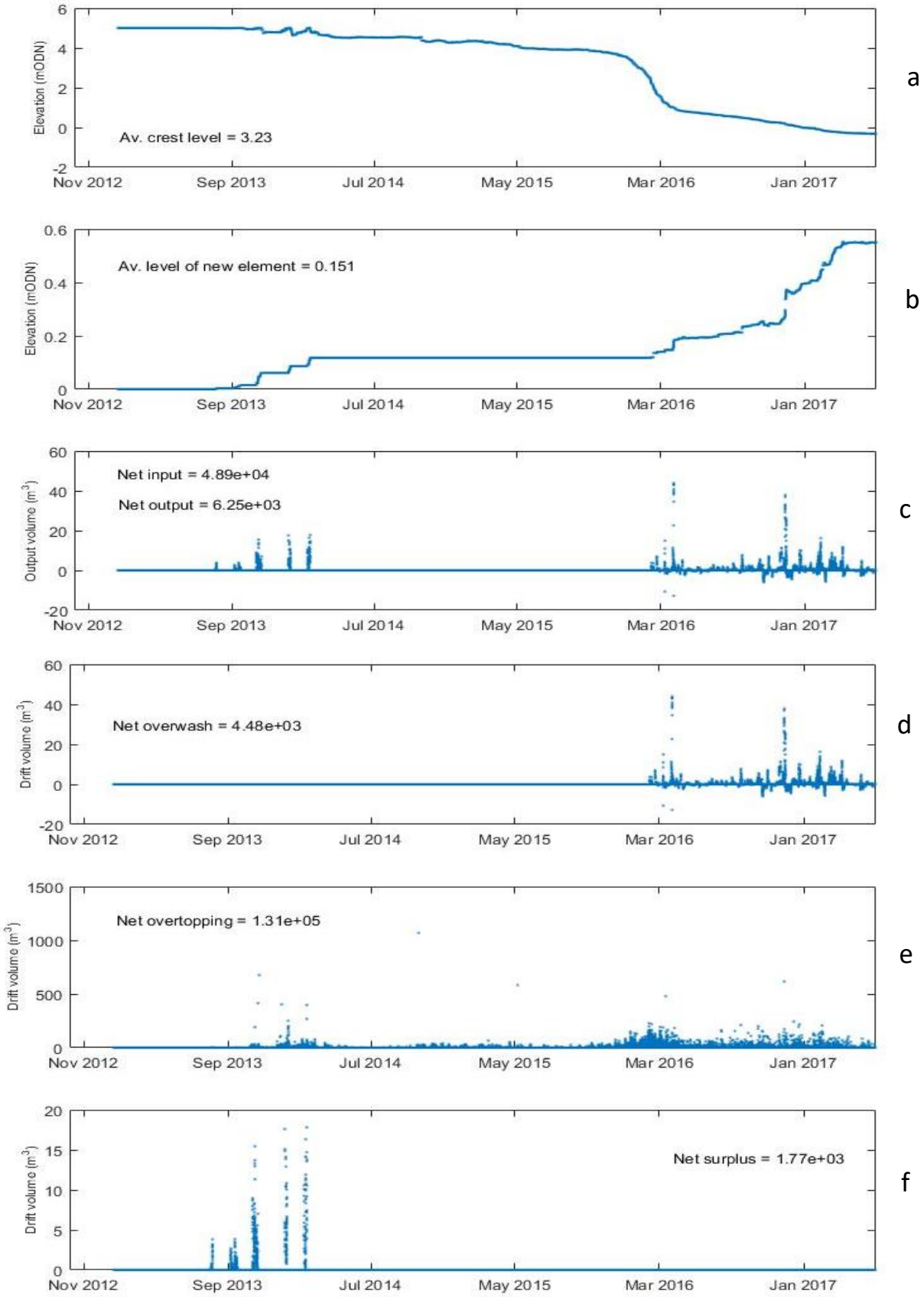

Figure 34- Sensitivity model run G: (a) Crest level; (b) Level of new element; (c) Net input and output; (d) Overwash volume; (e) Overtopping volume; (f) Surplus sediment volume.

When the crest width was doubled to 40 m in model run E (Figure 32), the average crest level increased by 49 %, while the net overtopping volume shown was an order of magnitude lower. No overwash occurred in this model run. In comparison, when the crest width was halved to 10 m in model run D (Figure 31), there was a 46.5 % reduction in the average crest level and an increase of $1.33x10^4$ m^3 was shown in the net overwash volume. Similar values were obtained for the net surplus volume and overtopping volume when the crest width was halved.

By increasing the spit slope gradient from 1:6 to 1:4 in model run F (Figure 33), the average crest level increased by 1.01 m and the net overtopping volume, despite being marginally lower, was on the same order of magnitude. However, the net overwash volume lowered by over an order of magnitude. Decreasing the spit slope gradient from 1:6 to 1:8 in model run G (Figure 34), displayed similar results, with similar net overwash and overtopping volumes and the average crest level increased by only 0.04 m.

4. Discussion

This section of the thesis has been split into four main segments to focus on the overall aims of the project. The first segment will discuss the recent morphological changes that have taken place at Pagham Harbour entrance since 2015, while the second segment will discuss the climatic conditions over this period. The third and fourth segments will then discuss the potential causes of the breach in 2016 and how the overtopping-overwash spit model can contribute to our understanding of the changes that have taken place.

4.1. Morphological evolution of the spit system and inlet entrance

The morphological changes of the Pagham Harbour frontage are examined by considering the progressive breakdown of the Church Norton spit, the subsequent migration of the detached spit downdrift of the breach and how these changes have affected the beach volumes in the area.

4.1.1. Progressive breakdown of the Church Norton spit

As previously mentioned, a breach occurred along the Church Norton spit early in 2016. In the few years leading up to this breach event as explored by this study, the south coast was subjected to a sequence of intense storm activity, particularly during the winter of 2013/2014. However, this raises the question as to why the spit did not breach during the winter of 2013/2014, which was characterised by the most intense storm activity and instead breached two winters later, during the winter of 2015/2016.

In the GIS analysis, the Church Norton spit displayed evidence of the progressive breakdown of a section of the barrier, indicated by a reduction in the total volume of sediment in cells E, F and G. A previous study on barrier breakdown by Pye and Blott (2009), found that barrier breakdown could be initiated in periods of intense wave attack combined with high water levels. Applying this finding to the Church Norton spit, the intense and sustained wave attack observed during the winter storms of 2013/2014, in combination with high water levels, could therefore explain the onset of this progressive breakdown shown along the central section of the spit. This behaviour displayed by Church Norton spit was comparable to the behaviour shown by the Dunwich-Walberswick gravel barrier in Suffolk, whereby there was a progressive breakdown of a section of the barrier (Pye and Blott, 2009).

Relating this finding from the GIS analysis to the results obtained from the breach mechanism model, the first two episodic lowering events shown in the model may have acted to weaken the crest. Although material was likely to have been moved offshore during the events as the beach profile adjusted towards a new equilibrium, this was likely to be only temporary (Donnelly *et al.,* 2006). Most

of the material was likely transported back onshore by shoaling waves, in the brief period after (Masselink and van Heteren, 2014). However, during the intense storm event that occurred on 14/02/2014, known as the Valentine's Day storm, it is likely that a considerable volume of sediment was moved offshore and lost, hence the barrier was unable to recover to a sustainable crest elevation (Pye and Blott, 2009).

Additionally, the small reduction in the volume of spit sub-cells E, F and G above 0 m ODN provides an indication of overwashing and the potential deposition of material in washover fans, landward of the spit and outside the area defined by the spit sub-cells (Stripling *et al.,* 2008), or slumping. The process of overwashing is discussed further in Section 4.3.

4.1.2. Migration of detached spit

Influenced by the combination of wave activity and tidal flow through the newly formed inlet channel, the detached spit moved progressively shoreward, as it migrated alongshore across cells H to J. An earlier study by Aubrey and Gaines (1982), on the migration of a detached body of sediment similar to that observed at Pagham, suggested that it occurred either through overwashing and gradual rollover of the barrier or by truncation of the distal ends. The largest volume changes observed below 0 m ODN suggest how as the detached spit migrated, it filled accommodation space in the former main inlet channel and hence formed a platform from which the detached supra-tidal spit could then prograde (Townend, 2015).

4.1.3. Variation in beach profile volume

Despite the rate of littoral drift reducing since 2014, the profiles immediately downdrift have shown a general increase in volume post-breach. This is most likely attributed to the area immediately downdrift being nourished with material supplied from the detached spit, as it merged to the shoreline. Furthermore, the rapid decrease in area per unit width observed in profile P4d01391 coincides with the general location of the new inlet channel, formed initially by the breach, but matured through tidal flow as the detached spit migrated downdrift.

It is clear however, that there was a gradual lowering in the volume of profiles updrift since at least 2012 and perhaps before, although this is outside the temporal scope of this study. This provides the first indication that there may have been a reduction in the sediment supply available to the Church Norton spit over this extended period and highlights the potentially increasing vulnerability of the spit leading up into winter 2015/2016.

4.2. Importance of the climate conditions

4.2.1. Wave climate

During the winter of 2013/2014, the south coast of the UK was subjected to an exceptionally high number of intense storm events from the Atlantic (Masselink *et al.,* 2015). Similarly, during the winter of 2015/2016, the coast was again subjected to a period of intense storm activity, although not quite to the same extreme levels.

When considering the peak wave period, both winter 2013/2014 and winter 2015/2016 were characterised by notably high peak wave periods. A previous study by Bradbury and Powell (1992) on the response of a shingle spit to wave action found that as the wave period increased, provided there was insufficient sediment available to raise the crest, the frequency of overwashing also increased because of the greater volume of water contained within longer period waves. In 2015/2016, the combination of the lower rate of littoral drift and the progressive reduction in volume across the central section of the spit reduced the sediment availability, enough to allow an increase in the rate of overwash to occur. Additionally, due to the reflective nature of a shingle barrier, when longer period waves occur in the nearshore wave climate, as shown in winter 2013/2014 and 2015/2016, the sub-harmonic component can be amplified, therefore offering a mechanism by which the run up can be extended over the crest (Carter and Orford, 1984). The combination of this mechanism with larger wave heights could have also led to increased overtopping, resulting in the landward slope slumping and a reduction in the elevation of the crest.

Wave period is also an important parameter to consider when assessing wave energy fluxes and storm activity. This is because the wave energy flux can double when the wave period doubles, as the wave energy flux is a function of both the wave period and height (Masselink *et al.*, 2015). Both winter 2013/2014 and 2015/2016 were characterised by notable peaks in the inshore energy flux, coinciding with substantial peaks in monthly littoral drift volumes, because the longshore component of energy flux is proportional to littoral drift (Komar and Inman, 1970). However, the mean monthly drift volumes over winter 2013/2014 were fractionally higher, due to a higher inshore energy flux resulting from the exceptionally intense storm activity over that period.

In terms of significant wave height, this may have affected the position of the crest. During extended periods of higher significant wave heights, characteristic of the storms that occurred in winter 2013/2014 and 2015/2016, the crest may have retreated landwards due to the processes of erosion and steepening, resulting in subsequent slope failure of the seaward face. Upon reaching a minimum crest width, flow through the shingle barrier may have also triggered slope failure and breach development (Obhrai *et al.,* 2008). Similarly, no notable variation in wave direction was shown to

occur between winter 2013/2014 and winter 2015/2016 and the Pagham coastline subjected to storms predominantly from the south-westerly direction. This highlights the importance of the antecedent morphology, in addition to wave and tidal forcing, on the morphological response of a beach to storms (Ruiz de Alegria-Arzaburu and Masselink, 2010).

Taking this into account and considering the wave climate alone, the storm activity experienced during the winter of 2015/2016 was not likely to have initiated the breach. This suggests that there were other key factors exerting a control on the timing of the breach.

4.2.2. Importance of antecedent morphology

The stability of the shingle barrier and the likelihood of a subsequent breach, not only require the consideration of storm events and highwater levels, but must further consider the alongshore sediment transport and antecedent morphology (Matias *et al.* 2012). As water will take the path of minimum resistance, the critical factor determining the location of a breach is the antecedent height along the barrier (Basco and Shin, 1999). For the Church Norton spit, this was spatially non-uniform, with small discontinuities occurring along a central section of the crest, therefore displaying evidence of barrier preconditioning from previous storms events, most likely during winter 2013/2014 (Masselink and van Heteren, 2014). These sections of lower elevation could indicate localised areas where overwashing may have occurred previously or where wave energy may have been focused (Carter *et al*., 1987; Donnelly *et al.,* 2006). Preconditioning of a barrier can act to reduce the resilience of the spit barrier to storm events (Masselink and van Heteren, 2014) and subsequently the pre-conditioned areas would be increasingly susceptible to overtopping and overwashing (Bradbury and Powell, 1992). Further to this, progressive overwashing events would have the ability to exploit these discontinuities further, resulting in the development of breach (Donnelly *et al.,* 2006).

Additionally, there is a further point of interest regarding accommodation space. The lowering of the lower foreshore, as indicated below 0 m ODN over spit sub-cells E to G, may have allowed larger waves to propagate further shoreward and reach the spit. The lowering could suggest that a larger proportion of the littoral sediment supply was required to fill this accommodation space and effectively rebuild the platform on which the spit was built, rather than contributing material towards maintaining the crest height or even spit progradation.

4.2.3. Influence of littoral drift on the timing of the breach

The stability of drift-aligned barrier beaches such as the Church Norton spit, are known to be intrinsically unstable as they rely on a continued input of sediment from alongshore (Stripling *et*

*al.,*2008). The distribution of shingle alongshore via longshore sediment transport processes can therefore exert an important control on the barrier system dynamics (Matias *et al.*, 2012).

Previous studies on this section of coastline describe the alongshore migration of large shingle spurs, orientated perpendicular to the coastline, which form the main route for the transport of shingle onshore (Townend, 2015). Although the volume contained in these spurs was not found to be particularly large above -1 m ODN, the variability in the annual littoral drift volumes obtained appeared to partially coincide with the episodic input of material from the spurs, as they merged to the Church Norton spit after migrating along the coast (Townend, 2015). This most likely explains the considerably higher littoral drift potential shown in 2014 and suggests that despite the intense storm activity that occurred during the winter of 2013/2014, littoral drift rates were high enough to maintain the spit volume over this period. However, a decrease in annual littoral drift volumes and therefore a reduction in sediment supply can imped barrier recovery (Forbes *et al.,* 2004) and prevent the crest height being maintained, with respect to tidal levels (Stripling *et al.,* 2008). The decrease in the annual littoral drift volumes shown after 2014, may have subsequently made the shingle spit more vulnerable to overwashing processes in this period and limited the opportunities for barrier recovery.

4.2.4. Variation in longshore to cross-shore transport

The substantial increase shown in the LsXs ratio between October 2015 and November 2015 indicated either a decrease in cross-shore transport component, an increase in the longshore transport component, or a combination both over this period. However, it could most likely be attributed to the increase in the longshore transport component, as this would agree with higher monthly drift volumes obtained as the longshore component of energy flux proportional to littoral drift (Komar and Inman, 1970). Similarly, the smaller fluctuation in the ratio around 0.6, displayed in winter 2013/14 when also considering October and November 2013, suggests a larger longshore component. Whereas the reduction in the LsXs ratio shown after December 2016 indicated an increase in the cross-shore transport component, suggesting that storm-driven offshore direct sediment transport may have occurred (Masselink *et al.,* 2015).

4.3. Cause of the breach

4.3.1. Crest thinning

The crest width forms another key factor influencing the response of the spit crest to wave action (Bradbury and Powell, 1992). During a storm, a reduction in the width of the shingle crest can occur as the beach profile readjusts to reach dynamic equilibrium for the given storm conditions, provided there is sufficient sediment supply. As a result, the beach crest can be undermined and subsequently thinned (Bradbury and Powell, 1992). The narrow central section of the spit observed in this GIS analysis was likely an artefact of sustained wave attack in previous storm events (Scott and Townend, 2017), outside the temporal scope of this particular GIS study. However, a reduction in the crest width over a section of a spit can be indicative of a low sediment supply (Timmons *et al.,* 2010) and highlights the increasing vulnerability of this section of the spit crest to overtopping and overwash processes. A narrower spit is less effective as a barrier and more susceptible to damage during storm events (Aubrey and Gaines, 1982). Additionally, channels cutting through the beach crest have the potential to develop quicker in narrower crests, due to the acceleration of overwash on the steeper backslope (Donnelly *et al.,* 2006).

4.3.2. Crest lowering

The rate at which the crest lowered was a function of both the hydraulic conditions and the width of the crest (Donnelly *et al.,* 2006) and the likely mechanism incorporated both overtopping and overwashing. In comparison to finer grained barriers, the steeper seaward profile, reflective nature and high permeability make overtopping typical of shingle barriers, under the right combination of beach geometry, wave conditions and water levels (Stripling *et al.,* 2008). Orford *et al.* (2003) previously described the process of crest lowering as a positive feedback loop, whereby the reduction in crest height over a section of a barrier increases the likelihood of waves reaching the lowered crest, increasing the frequency of overwashing and hence reducing the crest height further (Bradbury, 1998).

As previously described prior to the breach, a central section of the spit showed evidence of roll back. Roll back can be caused by waves exceeding the crest limit and leading to a reduction in the crest elevation (Bradbury, 2000). The overtopping-overwash spit model suggests that a major sequence of overtopping events occurred in both the winter of 2013/2014 and 2015/2016. In the latter however, the model suggested a greater frequency of overtopping events because the wave energy requirement to overtop the lowered crest was reduced and hence the rate of lowering could increase further (Nicholls, 1985). The model further suggests that once the crest level had decreased to a critical threshold for the given wave and water level conditions, overwashing was initiated and a

subsequent acceleration in the reduction of the crest level occurred, as the low section through the crest was exploited. Once the crest had been reduced to a sufficient elevation where a breach could occur, a new inlet channel could then form at this location, developing through scouring processes by the tidal flows (Basco and Shin, 1999; Carter and Orford, 1981).

In comparison, the model suggests that no overwashing occurred in winter 2013/2014. This indicates that despite the intense storm activity experienced that winter and the small episodic fluctuations in the crest level suggested in the model, the crest level never reduced to an elevation where overwashing could occur. The water levels that occurred during these dates of episodic crestal lowering were all lower than the corresponding reduced crest heights. The recovery of the crest, as inferred from this model, following the episodic lowering events which occurred in winter 2013/2014 could be explained by a negative feedback loop, where overtopping was acting to raise the crest (Matias *et al.,* 2012). In the short-term, these negative feedback loops can reduce the possibility of overwash occurring, however in the longer term, it can increase the vulnerability of the crest due to the decrease in width and steeper profile (Orford *et al*., 2003). The occurrence of overtopping events suggested by the model throughout 2014 and 2015, but no overtopping events indicated prior to winter 2013/2014, further suggest that the crest may have become increasingly susceptible to overtopping following winter 2013/2014.

4.4. Overtopping and overwash model sensitivity

The following section will discuss the results obtained from the sensitivity analysis carried out on the overtopping and overwash spit model.

4.4.1. Effect of crest width

This overtopping and overwash model highlights the sensitivity of a barrier to variations in crest width and indicates the importance of this parameter when considering how the barrier responds to wave action (Bradbury and Powell, 1992). Despite the same freeboard, barriers with a large cross-sectional area are less likely to lower through overwash compared to barriers with a smaller cross-sectional area (Bradbury *et al., 2005*). The model results suggest that the narrower crest, the quicker the crest could lower because more waves could overtop the spit, leading to an increase in overtopping and therefore a breach could initiate more rapidly (Bradbury and Powell, 1992).

4.4.2. Effect of spit slope

The steeper spit slope and hence the greater water depth at the toe of the spit (Bradbury *et al., 2005*), enabled the onset of wave transformation and breaking to occur further landward than would otherwise occur with a shallower slope gradient. This subsequently reduced the width of the surf

zone and lead to the concentration of wave energy dissipation nearer the shoreline (Austin and Masselink, 2006). Normally the higher rates of infiltration in a gravel beach combined with a steeper slope, generally generate greater run-up and therefore increase the likelihood of overtopping (Matias *et al.* 2012). In this case however, the similar overtopping volumes obtained for model runs F and G suggest that slope had a negligible effect on overtopping. Additionally, there is a balance between runup able to generate overwash and transport sediment onto the landward slope of the spit and runup able to cause overtopping and hence deposit sediment at the crest (Matias *et al.*, 2012).

4.4.3. Variation of the overtopping transport coefficient

The model suggests that by increasing K_0, there was an increase in the volume of sediment lost through overtopping, which subsequently caused the crest level to reduce earlier and hence overwash could occur sooner (Bradbury, 1998). On the other hand, the model suggests that the reduction in K_0 reduced the amount of sediment lost through overtopping and hence the elevation of the crest remained generally higher for a longer period before rapidly decreasing. The high crest elevation would have had a higher energy requirement to overtop and therefore overtopping was less frequent (Nicholls 1985). As a result, there was a reduction in surplus material available to the feed the downdrift cell.

5. Conclusion

This section will review the hypotheses defined at the start of this thesis, discuss the wider significance of these results and address the limitations of this study and provide recommendations for future work on Pagham Harbour entrance.

5.1. Review of hypotheses

Hypothesis 1: The breach along Church Norton spit in spring 2016, was initiated through the lowering of the crest by storm action, and developed into a full breach through tidal action.

Hypothesis 2: The southern spit is reforming post breach and the relic Church Norton spit is migrating downdrift.

5.1.1. Hypothesis 1

The results from this study support the hypothesis that the crest was lowered via a combination of overtopping and overwashing events during storm activity. However, the main conclusion that can be drawn from this study is that the winter storm events of 2013/2014 appeared to act as a trigger to the breach that occurred early in 2016. The results suggest that the intense degree of storm activity experienced during winter 2013/2014 damaged the spit to the point where overtopping events could then occur frequently over the following year, including overtopping events during summer storm activity. As a result, by the start of winter 2015/2016 the Church Norton spit was in a particularly vulnerable morphological position to future storm events, as the spit was unable to fully recover due to lower littoral drift rates and hence the reduction in sediment supply. However, due to time limitation, further work needs to be undertaken to investigate the influence of tidal action on breach development.

5.1.2. Hypothesis 2

The results from the GIS analyses partially agree with this hypothesis. The results indicated that the relic Church Norton spit migrated in a downdrift direction, fusing with the shoreline in front of Pagham. In doing so, the beach immediately downdrift of the breach was fed with sediment and profiles over this area did show initial signs of recovery, due to the slight increase in beach volume. Over a timescale of a few months, this is likely to continue to have a positive effect on the downdrift coastline and address the erosional issues along Pagham frontage, even if only temporary, as the detached spit material is transported further alongshore. However, in terms of the reformation of the southern spit there is disagreement with this hypothesis. The results from the contour analysis showed that following the breach, the relic southern spit continued to recede in a south-westerly

direction as the breach gap widened and showed no sign of prograding and reforming. This suggests that there was insufficient sediment available to fed the re-growth of the spit over this period. However, in the future there could be the opportunity for the Church Norton spit to reform if sufficient sediment becomes available.

5.2. Wider importance of findings

On a local scale, the observed morphological behaviour from this study combined with the behaviour observed in earlier studies, can be used to infer how the site will behave in the future under different conditions and hence be used to inform future management schemes on site. However, on a wider scale, these findings are important, not only because they will contribute to the limited number of morphological studies conducted on gravel tidal inlets currently, but also because of the further understanding in barrier breakdown and spit breach development. These ideas relating to storm pre-conditioning and storm event triggers, are likely transferable to other gravel tidal inlets and barrier systems around the world, which may be displaying similar behaviour to that shown at Pagham.

5.3. Limitations of study

The key limitation with this study is the frequency of topographic baseline surveys conducted over the study site over this study period. Preferably additional topographic surveys, covering the periods both prior to and after the breach, would have been beneficial in order to increase the temporal resolution of the morphological behaviour displayed. One would then be able to identify any morphological changes occurring over shorter time intervals, which may not have previously been observed. Furthermore, the overtopping-overwash model used to model the breach development was a highly simplified representation and only provides an indication of the effect that these processes have on the crest level. The parameters defined in this model only provide an approximation for the spit crest geometry and do not account for more complex swash formed morphology, common to gravel beaches, such as berms. In hindsight, I should have also extended the wave climate timeseries back further, prior to 2012, to be able to observe the longer running patterns in the wave climate.

5.4. Future of Pagham Harbour entrance

In June 2017 ABPmer, on behalf of the Pagham community, were granted planning permission to manage the Church Norton spit fronting Pagham Harbour. The approved scheme will involve diverting tidal energy away from areas of the beach that have shown to be particularly vulnerable to erosion, by managing the spit shape (ABPmer, 2017).

5.5. Future project work

There is scope for further research in many areas related to this project. Firstly, future project work could investigate why the breach occurred at the point it did along the Church Norton spit. It would also be interesting to re-analyse the wave data from the Rustington wave buoy, to identify storm and swell wave activity and then investigate the morphological response of Church Norton spit and the surrounding coastline to swell and storm waves. Additionally, it would be useful to extend the overtopping-overwash spit model back over the period prior to 2013, using the same K_0 value of 17 and an initial crest height of 0 m ODN, to see if the spit builds up to the observed crest level. A future project could also use a more sophisticated model, for example the Aggregated Scale Morphological Interaction between a Tidal basin and the Adjacent coast model (ASMITA), to further explore the dynamic spit behaviour shown at Pagham, by producing a more detailed model of volume change which could then be compared to the GIS analysis.

6. References

ABPmer. 2017. ABPmer delighted with Planning Permission approval for shingle spit management at Pagham Harbour. [Online] Available: http://www.abpmer.co.uk/buzz/abpmer-delighted-with-planning-permission-approval-for-shingle-spit-management-at-pagham-harbour/. [Accessed 16/08/2017].

ABPmer. 2015. Managed Breach of Shingle Spit at Pagham: Proposal Design and Modelling Report. Report R.2404. *Report to Pagham Parish Council*.

Anthony, A. J. 2008. Shore Processes and their Palaeoenvironmental Applications. *Developments in Marine Geology*. 4.

Aubrey, D.G. and Gaines, A.G. 1982. Rapid formation and degradation of barrier spits in areas with low rates of littoral drift. *Marine Geology*. 49. 257-278.

Austin, M.J. and Masselink, G. 2006. Observations of morphological change and sediment transport on a steep gravel beach. *Marine Geology*. 229. 59-77.

Barcock, N.W.S and Collins, M.B. 1991. Coastal erosion associated with a tidal inlet: Pagham, West Sussex. Report to Arun District Council and National Rivers Authority. *University of Southampton*. Southampton.

Basco, D.R. and Shin, C.S. 1999. A One-Dimensional Numerical Model for Storm-Breaching of Barrier Islands. *Journal of Coastal Research*. 15. 241-260.

Blott, S.J. and Pye, K. 2001. GRADISTAT: a grain size distribution and statistics package for the analysis of unconsolidated sediments. *Earth Surface Processes and Landforms*. 26. 1237-1248.

Bradbury, A.P. 2000. Predicting Breaching of Shingle Barrier Beaches - Recent Advances to Aid Beach Management. [Online] Available: https://www.newforest.gov.uk/media/adobe/9/l/PREDICTING_BREACHING_OF_SHINGLE_BARRIER_BEACHES.pdf [Accessed 14/08/2017].

Bradbury, A.P. 1998. Response of Shingle Barrier Beaches to Extreme Hydrodynamic Conditions. unpublished PhD thesis. School of Ocean and Earth Science. University of Southampton. 309.

Bradbury, A.P., Cope, S.N. and Prouty, D.B. 2005. Predicting the response of shingle barrier beaches under extreme wave and water level conditions in southern England. *Fifth International Conference on Coastal Dynamics, April 4-8, Barcelona,* Spain.

Bradbury, A.P. and Powell, K.A. 1992. The Short Term Profile Response of Shingle Spits to Storm Wave Action. *Coastal Engineering Proceedings*. 23. 2694-2707.

Bray, M.J., Carter, D.J. and Hooke, J.M. 1995. Littoral Cell Definition and Budgets for Central Southern England. *Journal of Coastal Research*. 11. 381-400.

Bruun, P. and Gerritsen, F. 1959. Natural bypassing of sand at coastal inlets. *Journal of Waterways and Harbours Division*. 85. 75-107.

Burningham, H. and French, J. 2006. Morphodynamic behaviour of a mixed sand-gravel ebb-tidal delta: Deben estuary, Suffolk, UK. *Marine Geology*. 225. 23-44.

Carter, R.W.G. and Orford, J.D. 1984. Coarse Clastic Barrier Beaches: A Discussion Of The Distinctive Dynamic And Morphosedimentary Characteristics. *Marine Geology.* 60. 377-389.

Carter, R.W.G. and Orford, J.D. 1981. Overwash processes along a gravel beach in south-east Ireland. *Earth Surface Processes and Landforms*. 6. 413-426.

Carter, R.W.G., Orford, J.D., Forbes, D.L. and Taylor, K.B. 1987. Gravel barriers headlands and lagoons: an evolutionary model. *Coastal Sediments 1987 ASCE*. 2. 1776-1792.

Cooper, N.J. and Pontee, N.I. 2006. Appraisal and evolution of the littoral 'sediment cell' concept in applied coastal management: Experiences from England and Wales. *Ocean and Coastal Management*. 49. 498-510.

Cope, S.N. 2004. Breaching of UK Coarse-clastic Barrier Beach Systems: Methods developed for predicting breach occurrence, stability and flooded hinterland evolution. *PhD thesis. Department of Geography. University of Portsmouth*.

Cundy, A.B., Long, A.J., Hill, C.T., Spencer, C. and Croudace, I.W. 2002. Sedimentary response of Pagham Harbour, southern England to barrier breaching in AD 1910. *Geomorphology*. 46. 163-176.

Donnelly, C., Kraus, N. and Larson, M. 2006. State of Knowledge on Measurement and Modelling of Coastal Overwash. *Journal of Coastal Research*. 22. 965-991.

FitzGerald, D.M. 1988. Shoreline erosional-depositional processes associated with tidal inlets. Hydrodynamics and Sediment Dynamics of Tidal Inlets. *Springer-Verlag. New York.* 186-225.

FitzGerald, D.M., Kraus, N.C. and Hands, E.B. 2000. Natural Mechanisms of Sediment Bypassing at Tidal Inlets. US Army Corps of Engineers. Coastal Hydraulics Laboratory. Vicksburg. MS. Report ERDC/CHL CHETN-IV-30.

Forbes, D.L., Parkes, G.S., Manson, G.K. and Ketch, L.A. 2004. Storms and shoreline retreat in the southern Gulf of St. Lawrence. *Marine Geology*. 210. 169-204.

Gao, S. and Collins, M. 1994. Tidal Inlet Equilibrium, in Relation to Cross-sectional Area and Sediment Transport Patterns. *Estuarine, Coastal and Shelf Science*. 38. 157-172.

Hayes, M.O. 1969. Coastal Environments: NE Massachusetts and New Hampshire. Guidebook, Fieldtrip for Eastern Section of SEPM. May 9-11. 462pp.

Hayes, M.O. 1980. General morphology and sediment patterns in tidal inlets. *Sedimentary Geology*. 26. 139-156.

HR Wallingford. 1995. Pagham to Portsmouth Harbour (Coastal) Strategy Study. Report EX 3121. *Report to Pagham to River Hamble Coastal Group.*

Kirk, R.M. 1980. Mixed sand and gravel beaches: morphology, processes and sediments. *Progress in Physical Geography*. 4. 189-210.

Komar, P.D. and Inman, D.L. 1970. Longshore Sand Transport on Beaches. *Journal of Geophysical Research*. 75. 5914-5927.

Masselink, G. and Russell, P. 2013. Impacts of Climate Change on Coastal Erosion. Marine Climate Change Impacts Partnership: *Science Review*. 71-86.

Masselink, G., Scott, T., Poate, T., Russell, P., Davidson, M. and Conley, D. 2015. The extreme 2013/2014 winter storms: hydrodynamic forcing and coastal response along the southwest coast of England. *Earth Surface Processes and Landforms*. 41. 378-391.

Masselink, G. and Van Heteren, S. 2014. Response of wave-dominated and mixed-energy barriers to storms. *Marine Geology*. 352. 321-347.

Matias, A., Williams, J.J., Masselink, G. and Ferreira, O. 2012. Overwash threshold for gravel barriers. *Coastal Engineering*. 63. 48-61.

McCall, R.T., Masselink, G., Poate, T.G., Bradbury, A.P., Russel, P.E. and Davidson, M.A. 2013. Predicting overwash on gravel barriers. *Journal of Coastal Research*. 65. 1473-1478.

Nicholls, R.J. 1985. The Stability of Shingle Beaches in the Eastern Half of Christchurch Bay. Unpublished PhD thesis. Department of Civil Engineering. University of Southampton. 468.

Obhrai, C., Powell, K. and Bradbury, A. 2008. A laboratory study of overtopping and breaching of shingle barrier beaches. *International Conference on Coastal Engineering 2008, 31 Aug-5 Sept, Hamburg,* Germany.

Orford, J., Jennings, S. and Pethick, J. 2003. Extreme storm effect on gravel dominated barriers. *Proceedings Coastal Sediments 2003*. *Corpus Christi*, Texas.

Owen, M.W. 1980. Design of seawalls allowing for wave overtopping, Report No: EX 924, Ltd H R, Wallingford.

Pye, K. 2001. The Nature and Geomorphology of Coastal Shingle. In Part 1: Geomorphology, Sediment Dynamics, Hydrology and Soils. In: Packham, J. R. Randall, R. E. Barnes, R. S. K. Neal, A. Ecology and Geomorphology of Coastal Shingle. *Westbury Academic and Scientific Publishing*. 2-22.

Pye, K. and Blott, S.J. 2009. Progressive Breakdown of a Gravel-Dominated Coastal Barrier, Dunwich-Walberswick, Suffolk, U.K.: Processes and Implications. *Journal of Coastal Research*. 25. 589-602.

Royal Haskoning. 2009. Pagham Coastal Defence Study Geomorphological Assessment. *Report to Arun District Council.*

Ruiz de Alegria-Arzaburu, A. and Masselink, G. 2010. Storm response and beach rotation on a gravel beach, Slapton Sands, U.K. *Marine Geology*. 278. 77-99.

Scott, C. and Townend, I. 2017. Pagham Harbour: Managing a dynamic coast for people and the environment. *Proceeding of Institution of Civil Engineers Coasts, Marine Structures and Breakwaters 2017 conference*. In Press.

Soulsby R, 1997, *Dynamics of marine sands*, Thomas Telford, London. 193-196.

Stripling, S., Bradbury, A.P., Cope, S.N. and Brampton, A.H. 2008. Understanding Barrier Beaches. R&D Technical Report FD1924/TR to Defra and Environment Agency Flood and Coastal Erosion Risk Management R&D Programme.

Timmons, E.A., Rodriguez, A.B., Mattheus, C.R. and DeWitt, R. 2010. Transition of a regressive to a transgressive barrier island due to back-barrier erosion, increased storminess and low sediment supply: Bogue Banks, North Carolina, USA. *Marine Geology*. 278. 100-114.

Townend, I.H. 2015. Brief Analysis of Pagham Spit Evolution. *Coastal Science and Engineering Applications*. 1-11.

Townend, I.H. 2016. CoastalTools Manual and Software. [Online] Available: www.coastalsea.uk [Accessed: 01/06/2017].

Van Rijn, L. C. Sutherland, J. 2011. Erosion of Gravel Barriers and Beaches. *Proceedings of Coastal Sediments 2011*. HR Wallingford. HRPP 501.

Velegrakis, A.F. 1994. Aspects of the morphology and sedimentology of a transgressional embayment system: Poole and Christchurch Bay, Southern England. *Unpublished Phd Thesis*. *Department of Oceanography. University of Southampton.*

Wentworth, C. K. 1922. A Scale of Grade and Class terms for Clastic Sediments. *Journal of Geology*. 5. 377-392.

Wright, L.D. and Short, A.D. 1984. Morphodynamic variability of surf zones and beaches: a synthesis. *Marine Geology*. 56. 93-118.